Effective Lagrangian at nonzero isospin chemical potential

A. Gómez Nicola* and A. Vioque-Rodríguez†
Universidad Complutense de Madrid, Facultad de Ciencias Físicas, Departamento de Física Teórica and IPARCOS, Plaza de las Ciencias 1, 28040 Madrid, Spain

(Received 23 September 2022; accepted 28 November 2022; published 19 December 2022)

We revisit the most general effective Lagrangian within chiral perturbation theory at nonzero isospin chemical potential μ_I up to $\mathcal{O}(p^4)$. In addition to the contributions already considered in the literature, we discuss the effects of new terms allowed by the symmetries derived within the external source method including spurion fields, as well as linear-field corrections relevant to $\mathcal{O}(p^4)$. We study the influence of those new contributions to the free energy density at zero temperature and observables derived from it, such as the pion and quark condensates and the isospin density. Corrections are shown to be compatible with lattice results, which favor nonzero values for the low-energy constants (LECs) multiplying the new $\mathcal{O}(p^2)$ and $\mathcal{O}(p^4)$ field operators in the Lagrangian. In particular, the $\mathcal{O}(p^4)$ LECs are renormalized to render the free energy density finite. Constraints on the LECs arise from preserving the physical condition $n_I(\mu_I < \mu_c) = 0$, while $\mu_c = M_\pi$ still holds to leading order and can be maintained to next-to-leading order through an additional constraint requiring the new LECs.

DOI: 10.1103/PhysRevD.106.114017

I. INTRODUCTION

The study of the QCD phase diagram has experienced a notable boost over the last decade, due to the advance of both lattice field theory at nonzero temperature and chemical potentials [1–6] and experimental data of relativistic heavy-ion collisions (RHICs) within the so-called Beam Energy Scan program probing the transition at chemical freeze-out [7,8].

Regarding chemical potentials, the main interest has been focused on the baryon chemical potential μ_B, motivated mostly by the possible existence of a critical point separating the $\mu_B = 0$ crossover transition from a first-order one [5,6]. However, the difficulties for the lattice analyses at $\mu_B \neq 0$ associated with the sign problem [4,9–12] have motivated the study of QCD when chemical potentials associated with additional, physically relevant charges are present, which do not present such a sign problem. This is the case of isospin μ_I and strangeness μ_S chemical potentials, which are actually relevant phenomenological quantities at RHICs at chemical freeze-out, related to electric charge and strangeness conservation [8,13]. Another example is the chemical potential μ_5 associated with chiral imbalance, which has been explored recently both in the lattice [14–16] and within effective theories [17,18]. The latter has been mainly motivated by the possible existence of local P-breaking regions within RHICs and related phenomena such as the chiral magnetic effect [19].

The case of isospin chemical potential μ_I has become particularly interesting. As it was first shown in [20] within a leading-order (LO) chiral perturbation theory (ChPT) effective theory approach, QCD at increasing μ_I exhibits a second-order phase transition from the normal vacuum phase to a Bose-Einstein condensation (BEC) phase for the charged pion modes. The transition point μ_c predicted by ChPT analyses is at the physical pion mass, including next-to-leading-order (NLO) corrections [21,22] which have extended to three flavors in [23]. For high enough μ_I, the system would enter a BCS-like phase [20] where effective theory approaches based on the low-density regime, such as ChPT, are expected to break down [24,25].

Other recent analyses at $\mu_I \neq 0$ have included finite temperature corrections, allowing one to study the effects on the QCD transition [22,26–29]. Temperature effects are expected to smooth out the BEC transition, increasing the value of the critical μ_I value for BEC, and setting an upper temperature limit for which the BEC phase no longer takes place. In addition, the QCD transition temperature T_c is expected to drop with increasing μ_I. Other effects considered in this context have been $\mu_B \neq 0$ [30] and $\mu_S \neq 0$ [31,32] corrections. A recent analysis within the Nambu-Jona-Lasinio (NJL) model confirms the ChPT results showing some deviations for $\mu_I \gtrsim 2M_\pi$ [33].

*gomez@ucm.es
†avioque@ucm.es

Lattice works are consistent with the previous findings. In particular, in [25] the free energy density as a function of the isospin density n_I, as well as n_I versus μ_I were investigated at a small but nonzero temperature of around $T \sim 20$ MeV. Significant deviations from the ChPT prediction take place for $\mu_I \gtrsim 2M_\pi$ and the ratio of the free energy density with the Stefan-Boltzmann free energy density corresponding to free quarks exhibits a maximum around $\mu_I \simeq 1.3\ M_\pi$, which was interpreted in [25] as the onset of the BEC phase. Such a peak behavior is well reproduced both within the ChPT and NJL approaches [33]. The apparent plateau of that ratio above $\mu_I = 3M_\pi$ might indicate a BEC-BCS crossover. On the other hand, lattice simulations at finite temperature and nonzero isospin chemical potential confirm the decreasing behavior of T_c with μ_I as well as the increase of the BEC onset with the temperature [34,35]. Recent analyses provide results for the pion and quark condensates from $T = 113$ MeV up to the QCD transition temperature, confirming those trends for the $T - \mu_I$ phase diagram [36,37]. Lattice results for n_I as a function of μ_I for low temperatures are provided in [38]. Recent comparisons between lattice data and the ChPT and NJL model approaches can be found, respectively, in [39] and [40].

In the context of lattice analyses, it is worth pointing out that the present uncertainties do not allow one to pin down μ_c around M_π. For instance, in [37] $\mu_c = M_\pi$ is actually imposed instead from the ChPT result commented above, in order to reduce uncertainties around the critical value. On the other hand, the results in [38] are compatible with a nonzero value for the isospin density below $\mu_I = M_\pi$, which would call for $\mu_c < M_\pi$.

In this work, we will discuss some new relevant aspects related to the formulation of the effective ChPT Lagrangian at nonzero isospin density. The usual approach to construct the effective Lagrangian follows from considering the isospin contribution in the QCD Lagrangian as an external constant vector source in the τ_3 direction and using the well-known external source method [41,42] so that the chemical potential enters through covariant derivatives rendering the theory locally invariant under the chiral symmetry. However, since the μ_I term in QCD is not invariant under isospin rotations in the $\tau_{1,2}$ directions, the most general effective Lagrangian may include additional terms with such a symmetry-breaking pattern, which would be multiplied by additional low-energy constants (LECs). A systematic procedure to account for all the possible terms of such a type is provided by the so-called spurion method, which is an extension of the external source method developed originally to include correctly the effects of the electromagnetic field in the chiral Lagrangian [43–46]. Following similar ideas, the most general chiral Lagrangian for $\mu_5 \neq 0$ has been derived up to $O(p^4)$ in [18]. In addition, we will see that certain terms coming from contributions linear in the pion fields at $\mu_i \neq 0$ do actually provide a new contribution to the free energy density at the order considered here.

Thus, the plan of the paper is as follows. In Sec. II, we will revisit the construction of the most general $\mu_I \neq 0$ effective Lagrangian up to $\mathcal{O}(p^4)$ including possible new terms of the type commented above. In Sec. III, we will calculate the free energy density up to NLO in the chiral expansion including the new terms in the $\mathcal{O}(p^2)$ and $\mathcal{O}(p^4)$ Lagrangians, as well as the new correction coming from the linear terms in the effective Lagrangian, not considered before, which also arises to NLO. Thus, in Sec. III A, we will analyze the contributions coming from the second-order Lagrangian $\mathcal{L}_2$, a first estimate of the numerical effect of the new corrections is carried out in Sec. III B, fitting the only undetermined parameter in $\mathcal{L}_2$ to lattice points, while in Sec. III C, all the NLO corrections to the free energy density will be included, both from the $\mathcal{O}(p^4)$ Lagrangian and from the linear term. In Sec. IV, we will analyze the constraints on the new LEC imposed by the vanishing of the isospin density below the critical point, as well as to what extent the condition $\mu_c = M_\pi$ is affected by the new terms up to NLO. Finally, in Sec. V, we will evaluate numerically our NLO results for the different observables obtained from the free energy density, calibrating the corrections coming from the new LEC and from the linear term, compared to lattice results.

In this paper, we will work for $SU(2)$ at $T = 0$ to obtain a first glance of those new effects, leaving the finite temperature and strangeness corrections for future work.

II. CHIRAL LAGRANGIAN INCLUDING EXPLICIT ISOSPIN-BREAKING OPERATORS

We start from the QCD Lagrangian including a nonzero isospin chemical potential corresponding to the grand-canonical partition function. The fermionic part of the Lagrangian reads

$$\mathcal{L}_{\mathrm{QCD}} = \bar{q}(i\not{D} - \mathcal{M})q + \frac{\mu_I}{2}\bar{q}\gamma_0\tau_3 q \tag{1}$$

with $q^T = (u, d)$, $\not{D}$ is the covariant derivative corresponding to the gluon field, $\mathcal{M}$ is the quark mass matrix, which here we take as $\mathcal{M} = m\mathbb{1}$ with $m = m_u = m_d$, and τ_k are the Pauli matrices.

The $\mu_I = 0$ Lagrangian is chiral invariant $SU(2)_L \times SU(2)_R$ for $\mathcal{M} = 0$ (chiral limit) which reduces to the isospin symmetry $SU(2)_V$ with $V = L = R$ for nonzero quark masses. However, for nonzero μ_I, the latter symmetry breaks down to $U(1)_{I_3}$ since the μ_I term is only invariant under vector transformations in the τ_3 direction. Note also that Lorentz invariance is also broken by the inclusion of the μ_I term, as a consequence of the preferred reference frame of the thermal bath at rest. In addition, the isospin chemical potential term breaks C invariance, since it is essentially a charge operator. Therefore, the low-energy effective Lagrangian must share the above symmetry requirements in the most general way. That is, at a given order in the chiral (low-energy) power counting, one must include all possible operators compatible with the symmetries and their breaking. This can be ensured by following the external source method, where the scalar, pseudoscalar, vector, and axial vector sources are space-time dependent to ensure local chiral invariance, as well as Lorentz, P, C invariance, of the QCD Lagrangian. The effective Lagrangian is then constructed out of the most general set of operators satisfying such an invariance at a given order in the generic momentum scale p, which accounts for meson masses and derivatives, as well as $\mu_I = \mathcal{O}(p)$ which limits the ChPT analysis to low and moderate values of μ_I, as discussed below.

An important comment is in order here. The building blocks for constructing such operators are in principle the Goldstone boson (GB) field operator codified in an $SU(2)$ matrix field U, its covariant derivative $d_\mu U$ including the external sources, as well as the flavor matrices entering those external sources, which in the case given by (1) are the mass matrix $\mathcal{M}$ and $\frac{\mu_I}{2}\tau_3$. The latter point, i.e., the fact that one can have additional operators including $\frac{\mu_I}{2}\tau_3$ in a compatible way with the symmetry pattern, is actually one of the main novelties of our present work. One can easily understand this by considering all possible operators to order $\mathcal{O}(p^2)$. In addition to the standard terms

$$\mathrm{Tr}[d_\mu U d^\mu U^\dagger], \mathrm{Tr}[\mathcal{M}(U + U^\dagger)], \tag{2}$$

the following independent term

$$\mathrm{Tr}[U\tau_3 U^\dagger \tau_3] \tag{3}$$

is also allowed since it breaks chiral symmetry but preserves $U(1)_{I_3}$ (see details below). Similarly, at $\mathcal{O}(p^4)$ there will be new operators allowed. The philosophy to include such additional terms is the same as when introducing electromagnetic corrections to the chiral Lagrangian [43] and the systematic procedure to account for all those terms consists of introducing the so-called "spurion" fields $Q_{L,R}(x)$ as additional space-dependent external sources transforming suitably under chiral transformations [18,43–46].

Let us explain this procedure in more detail for our present case. For that purpose, we cast the Lagrangian (1) in terms of external sources as

$$\mathcal{L}_{\mathrm{QCD}}[v_\mu, A_\mu Q, s] = i\bar{q}\not{D}q + \bar{q}\{[v_\mu(x) + A_\mu(x)Q(x)]\gamma^\mu - s(x) + i\gamma_5 p(x)\}q, \tag{4}$$

where $v_\mu \in SU(2)$. The above Lagrangian corresponds to the choice relevant for this work, $Q_L = Q_R = Q$, and we have set the axial source $a_\mu = 0$ with respect to the general source Lagrangian considered in [18,44–46], where we have kept a nonzero pseudoscalar source $p(x)$ in order to derive expectation values of pionic fields, such as the pion condensate.

The Lagrangian in (1) corresponds to the particular choice $v_\mu + A_\mu Q = \frac{\mu_I}{2}\tau_3$, $s = \mathcal{M}$, and $p = 0$. Thus, after the general effective Lagrangian is constructed, we will choose, without loss of generality,

$$v_\mu = 0, \qquad A_\mu = \Lambda\delta_{\mu 0}, \qquad Q = \frac{\mu_I}{2\Lambda}\tau_3, \tag{5}$$

consistent with our power counting as long as $\mu_I \ll \Lambda$. The choice of the parameter Λ is irrelevant, as it should be, since it will be absorbed in the new independent LEC involved, which will have to be determined. The important point is to include μ_I in the Q contribution, consistent with the counting $\mu_I = \mathcal{O}(p)$. In addition, as customary we will write $p(x) = j\tau_1$ so that taking derivatives with respect to j we reproduce expectation values of the π_1 field, which is the direction we have chosen for the condensed field.

The Lagrangian (4) can be made locally invariant under chiral $SU(2)_L \times SU(2)_R$ rotations of the quark and source fields. Here, it is enough to restrict to the vector subgroup $g_L = g_R = g \in SU(2)$, under which the Lagrangian in (4) can be made invariant by considering the following transformations:

$$\begin{aligned} &q(x) \to g(x)q(x), \\ &\chi(x) \to g(x)\chi(x)g^\dagger(x), \\ &v_\mu(x) \to g(x)v_\mu(x)g(x)^\dagger + ig(x)\partial_\mu g(x)^\dagger, \\ &Q(x) \to g(x)[Q(x)]g^\dagger(x) \end{aligned} \tag{6}$$

with $\chi(x) = 2B_0[s(x) + ip(x)]$. The constant B_0 was introduced in [41] and, as is customary, it is given by the relation $B_0 = M^2/(2m)$ with M the tree-level pion mass and m the quark mass. B_0 is also related to the quark condensate through the Gell-Mann-Oakes-Renner relation. In addition, one has to consider the C and P transformations of those fields given in [18,44–46] leading to a C and P invariant lagrangian.

The key point here is that the v_μ and $A_\mu Q$ sources can be transformed independently (we choose here to leave A_μ invariant for simplicity, which does not affect our arguments). As we are about to see, those spurion transformations are essential to ensure that all possible operators are accounted for.

Now, the chiral Lagrangian can be constructed order by order in the chiral expansion. The building blocks and their chiral counting are the pseudo-GB field $U \in SU(2)$, which is $\mathcal{O}(1)$, its covariant derivative

$$d_\mu U = \partial_\mu U + i[U, v_\mu + A_\mu Q], \tag{7}$$

which is $\mathcal{O}(p)$, and the external fields, which in this case are $\chi = \mathcal{O}(p^2)$ and $v_\mu = \mathcal{O}(p)$, $A_\mu Q = \mathcal{O}(p)$, where we follow the same convention as in [18,44–46] assigning the counting $A_\mu = \mathcal{O}(1)$, $Q = \mathcal{O}(p)$ as commented above. In addition, the following covariant derivative of the Q field

$$c_\mu Q = \partial_\mu Q - i[v_\mu, Q], \tag{8}$$

which is $\mathcal{O}(p^2)$, has to be formally considered, although in practice it will not enter our effective Lagrangian at the order considered here.

The chiral transformations of the U field, i.e., $U \to g_R U g_L^\dagger$, as well as those of the external sources and the covariant derivatives, and their C and P transformations, allow us to construct the most general effective Lagrangian which is locally chiral, C and P invariant for our present case. In particular, regarding the external sources, in addition to the usual corrections coming from the covariant derivative (7), which depends only on $v_\mu + A_\mu Q$, such as the first term in (2), additional terms are allowed, such as (3). That term comes from the invariant operator

$$\mathrm{Tr}[QUQU^\dagger],$$

which will be therefore multiplied by μ_I^2 times an independent LEC.

Let us now proceed order by order within this scheme following the discussion in [18], which considers all possible terms coming from arbitrary constant $Q_{L,R}$ fields. It is important to take into account that at the Lagrangian level, as customary, we will keep the $\mathcal{O}(p^n)$ notation to indicate the order of the field operators involved according to the counting we have just discussed. We will then classify the possible operators according to that counting, up to $\mathcal{O}(p^4)$. However, when referring to the free energy density and observables derived from it, we will use the equivalent parametric counting in inverse powers of F^2, where F is the tree-level pion decay constant. This distinction is pertinent because we will see below that physical constraints, such as the vanishing of the isospin density below μ_c, imply that certain low-energy constants or combinations of them are suppressed to a given order, which means that they do not count as the naive $\mathcal{O}(1)$ in the $1/F^2$ counting. Therefore, contributions to the free energy density multiplied by those constants will be formally of higher order, as we will see. Thus, at the lowest $\mathcal{O}(p^0)$ order, only trivial μ_I-independent terms can be constructed out of the U fields. At $\mathcal{O}(p)$ the only allowed structure is $\mathrm{Tr}(Q)$, which vanishes with the choice (5). To $\mathcal{O}(p^2)$, in addition to the structures (2) and (3), the terms $\mathrm{Tr}(Q^2)$ and $(\mathrm{Tr}Q)^2$ are also allowed, the latter vanishing with our choice (5). Therefore, the most general $\mathcal{O}(p^2)$ Lagrangian at nonzero μ_I is given by

$$\mathcal{L}_2 = \frac{F^2}{4}\mathrm{Tr}\left[d_\mu U d^\mu U^\dagger + \chi^\dagger U + \chi U^\dagger + \frac{1}{2}a_1\mu_I^2 U\tau_3 U^\dagger \tau_3\right] + \frac{1}{4}a_2 F^2 \mu_I^2, \tag{9}$$

where a_1 and a_2 are new low-energy constants to be determined below, and we have included an F^2 factor in front of the new terms just to render the new LEC dimensionless. As our analysis in Sec. IV A below will show, physical constraints imply that the actual chiral order of those constants has to be parametrically $a_{1,2} = \mathcal{O}(1/F^2)$ so that, as we just have explained, the contributions proportional to those constants will be formally of NLO.

It is also important to stress that, for the reasons already explained in terms of symmetry transformations, the Lagrangian contributions corresponding to the $a_{1,2}$ terms above are allowed independently. Actually, note that those two structures already appear in the derivative term through the covariant derivative, namely,

$$\mathrm{Tr}[d_\mu U^\dagger d^\mu U] = \mathrm{Tr}[\partial_\mu U^\dagger \partial^\mu U] + i\mu_I \mathrm{Tr}\{[\partial_0 U^\dagger, U]\tau_3\} - \frac{\mu_I^2}{2}\mathrm{Tr}[U^\dagger \tau_3 U \tau_3 - \tau_3^2], \tag{10}$$

where in the μ_I^2 term we recognize the a_1 and a_2 structures, respectively. However, as explained, this does not prevent those terms to be present independently in the Lagrangian, for the same reason as in the electromagnetic (EM) case, where the equivalent to the a_1 term gives rise to the EM pion mass difference. Actually, within the external field method with spurions, the origin of the $a_{1,2}$ new terms and those coming from the covariant derivative is completely different. Thus, while the $a_{1,2}$ terms contain explicitly the charge field Q but not the gauge field A_μ, only the combination $A_\mu Q$ enters in the covariant derivative term. It is only after making the replacement (5) that they have the same form.

In fact, the symmetry properties of the different terms in (10) are quite different. While the $\mu_I = 0$ and the U-independent terms are chiral invariant, the remaining ones are not, but remain $U(1)_{I_3}$ invariant. In addition, the term linear in μ_I breaks Lorentz covariance coming from A_μ and precisely the Lorentz structure of that term prevents it from being independently considered in the Lagrangian, which is not difficult to see following our derivation above. Other structures allowed within this formalism such as $\mathrm{Tr}F_{\mu\nu}F^{\mu\nu}$ vanish for a constant A_μ field.

Note also that the equations of motion (EOM) derived from the above Lagrangian are modified with respect to the $\mu_I = 0$ case as

$$(d_\mu d^\mu U^\dagger)U - U^\dagger d_\mu d^\mu U = \chi^\dagger U - U^\dagger \chi + \frac{1}{2}\mathrm{Tr}[U^\dagger \chi - \chi^\dagger U] - \frac{1}{2}a_1(U^\dagger \tau_3 U \tau_3 - \tau_3 U^\dagger \tau_3 U). \tag{11}$$

The above $\mathcal{O}(p^2)$ EOM can be used in the construction of the $\mathcal{O}(p^4)$ Lagrangian to eliminate some operators in favor of a minimal set [44] together with standard $SU(2)$ operator identities.

In principle, the following $\mathcal{O}(p^3)$ operators are also allowed [18]:

$$\begin{aligned}&\mathrm{Tr}(\chi^\dagger U+\chi U^\dagger)\mathrm{Tr}(Q),\quad \mathrm{Tr}(d_\mu U d^\mu U^\dagger)\mathrm{Tr}(Q),\\ &\mathrm{Tr}(QUQU^\dagger)\mathrm{Tr}(Q),\quad \mathrm{Tr}(Q^2)\mathrm{Tr}(Q),\quad [\mathrm{Tr}(Q)]^3,\end{aligned} \tag{12}$$

$$\begin{aligned}&\mathrm{Tr}[Q(d_\mu U d^\mu U^\dagger + d_\mu U^\dagger d^\mu U)],\quad \mathrm{Tr}[Q^2(UQU^\dagger+U^\dagger QU)],\\ &\mathrm{Tr}[Q(\chi^\dagger U+\chi U^\dagger+U\chi^\dagger+U^\dagger\chi)].\end{aligned} \tag{13}$$

The five operators in (12) vanish trivially with Q in (5). In addition, one can check that the operators in (13) also vanish for $d_\mu U$ and U in $SU(2)$ and Q in (5) as long as we remain in the isospin limit $m_u=m_d$, as we will do here consistently with isospin conservation. The last term in (13) is actually proportional to $\mathrm{Tr}(\tau_3\mathcal{M})=m_u-m_d$.

As for the $\mathcal{O}(p^4)$ Lagrangian, following the derivation in [18], we have in our present case

$$\begin{aligned}\mathcal{L}_4 &= \mathcal{L}_4^0+\mathcal{L}_4^Q,\\ \mathcal{L}_4^0 &= \frac{l_1}{4}[\mathrm{Tr}(d_\mu U d^\mu U^\dagger)]^2+\frac{l_2}{4}\mathrm{Tr}(d_\mu U d_\nu U^\dagger)\mathrm{Tr}(d^\mu U d_\nu U^\dagger)+\frac{l_3+l_4}{16}[\mathrm{Tr}(\chi^\dagger U+\chi U^\dagger)]^2+\frac{l_4}{8}\mathrm{Tr}(d_\mu U d^\mu U^\dagger)\mathrm{Tr}(\chi^\dagger U+\chi U^\dagger)\\ &\quad -\frac{l_7}{16}[\mathrm{Tr}(\chi^\dagger U-\chi U^\dagger)]^2+\frac{h_1+h_3-l_4}{4}\mathrm{Tr}(\chi^\dagger\chi)+\frac{h_1-h_3-l_4}{2}\mathrm{Re}\,\det\chi,\end{aligned} \tag{14}$$

$$\begin{aligned}\mathcal{L}_4^Q &= q_1\Lambda^2\mathrm{Tr}(d_\mu U d^\mu U^\dagger)\mathrm{Tr}(Q^2)+q_2\Lambda^2\mathrm{Tr}(d_\mu U d^\mu U^\dagger)\mathrm{Tr}(QUQU^\dagger)+q_3\Lambda^2[\mathrm{Tr}(d_\mu UQU^\dagger)\mathrm{Tr}(d^\mu UQU^\dagger)\\ &\quad +\mathrm{Tr}(d_\mu U^\dagger QU)\mathrm{Tr}(d^\mu U^\dagger QU)]+q_4\Lambda^2\mathrm{Tr}(d_\mu U^\dagger QU)\mathrm{Tr}(d^\mu UQU^\dagger)+q_5\Lambda^2\mathrm{Tr}(\chi^\dagger U+\chi U^\dagger)\mathrm{Tr}(Q^2)\\ &\quad +q_6\Lambda^2\mathrm{Tr}(\chi^\dagger U+\chi U^\dagger)\mathrm{Tr}(QUQU^\dagger)+q_7\Lambda^2\mathrm{Tr}[(\chi^\dagger U-U^\dagger\chi)QU^\dagger QU+(\chi U^\dagger-U\chi^\dagger)QUQU^\dagger]\\ &\quad +q_8\Lambda^4[\mathrm{Tr}(Q^2)]^2+q_9\Lambda^4\mathrm{Tr}(QUQU^\dagger)\mathrm{Tr}(Q^2)+q_{10}\Lambda^4[\mathrm{Tr}(QUQU^\dagger)]^2\end{aligned} \tag{15}$$

with Q in (5). The usual terms considered in the literature are included in the $\mathcal{L}_4^0$ Lagrangian, for which we have used the basis in [47],[1] whereas $\mathcal{L}_4^Q$ contains all possible operators including explicitly the Q field and whose influence on different observables will be analyzed in detail in Sec. III C. With respect to the basis considered in [21,22,29], the h_1 constant considered in those papers corresponds to h_1-l_4 here.

We emphasize that the additional terms in the Lagrangian in (9) and (15) are allowed for any physical system sharing the same symmetry pattern, like, e.g., the EM case. As we will see in Sec. IV, there are physical conditions which are specific to the $\mu_I\neq 0$ case which will give rise to constraints for those LECs. This is similar to other effective Lagrangian analyses which yield conditions for the LEC arising from different physical approximations, like vector meson dominance [43] or large N_c [42,48], which yield relations between LECs up to a given order.

Now, following also the derivation in [20–22,29], we allow for a nontrivial vacuum configuration of the GB field, which will parametrize the pion condensed phase. Namely, we write

$$\begin{aligned}U(x) &= A\,\exp\left[i\frac{\tau^a\pi^a(x)}{F}\right]A\\ A &= \cos(\alpha/2)\mathbb{1}+i\sin(\alpha/2)\tau_1\end{aligned} \tag{16}$$

with π^a the pion fields, so that the condensed phase is characterized by a nonzero value of the α angle, which is determined by minimizing the free energy density at a given chiral order, from which we will actually obtain the main properties of interest here. In the present work, we are interested in the free energy density at zero temperature, i.e.,

$$\epsilon(\mu_I,j)=-\lim_{T\to 0,V\to\infty}\frac{T}{V}\log Z(T,\mu_I,j)=\epsilon_2+\epsilon_4+\cdots, \tag{17}$$

where $Z(T,\mu_5)$ is the Euclidean partition function constructed out of the effective Lagrangian for nonzero μ_I, and ϵ_n is parametrically $\mathcal{O}(F^{4-n})$. Here we will consider it up to NLO, i.e., $\epsilon_2+\epsilon_4$. The above definition of the free energy density is equivalent to the effective potential considered in [20–22,29].

The observables of interest we can calculate in both phases are the quark and pion condensates and the isospin density, which are given, respectively, by

[1]In the basis used in [18], there is a typo in the LEC multiplying the $[\mathrm{Tr}(\chi^\dagger U-\chi U^\dagger)]^2$ operator in Eq. (4.1) in that paper, which should read $-(l_4+l_7)/16$.

$$\langle\bar{q}q\rangle(\mu_I) = \langle\bar{u}u + \bar{d}d\rangle = \frac{\partial\epsilon(\mu_I, j)}{\partial m} = 2B_0 \frac{\partial\epsilon(\mu_I, j)}{\partial M^2}, \quad (18)$$

$$\langle i\bar{q}\gamma_5\tau_1 q\rangle(\mu_I) = \frac{\partial\epsilon(\mu_I, j)}{\partial j} \quad (19)$$

$$n_I(\mu_I) = -\frac{\partial\epsilon(\mu_I, j)}{\partial\mu_I}. \quad (20)$$

III. FREE ENERGY DENSITY UP TO NEXT-TO-LEADING ORDER

A. Contributions from $\mathcal{L}_2$

The lowest order of the free energy density ϵ_2 is given just by minus the constant part of the $\mathcal{L}_2$ Lagrangian in (9):

$$\epsilon_2(\mu_I, j) = -\frac{F^2}{4}[\mu_I^2(1 + a_2 - (1 - a_1)\cos(2\alpha)) + 4M^2\cos\alpha + 8B_0 j\sin\alpha]. \quad (21)$$

At this order, the relevant observables can be calculated explicitly. For instance, the value α_0^{LO} minimizing the above expression with respect to α is given for $j = 0$ by

$$\cos\alpha_0^{(2)} = \begin{cases} 1 & \text{for } \mu_I < \mu_c = \frac{M}{\sqrt{1-a_1}}, \\ \frac{M^2}{(1-a_1)\mu_I^2} & \text{for } \mu_I > \mu_c, \end{cases} \quad (22)$$

where we use the (2) superscript to denote the contribution coming from ϵ_2 in (21). Therefore, the constant a_1 displaces the critical BEC value μ_c from the pion mass. We will see below that this is perfectly compatible, both with the effective Lagrangian framework and with lattice results, which will constrain the a_1 value and its uncertainty. In addition, as we will see in Sec. IV, $\mu_c = M$ holds formally to LO taking into account the chiral counting for a_1. Note also that the upper bound $a_1 < 1$ arises here from the very existence of a BEC phase.

The above result is also consistent with the modifications of the pion dispersion relations stemming from the μ_I-dependent Lagrangian above. In fact, let us consider the linear and quadratic terms in the pion field from the $\mathcal{L}_2$ Lagrangian in (9):

$$\mathcal{L}_2^{\text{lin}} = -F\sin\alpha[M^2 - (1 - a_1)\mu_I^2\cos\alpha]\pi_1(x) + F\mu_I\partial_0\pi_2(x)\sin\alpha + 2B_0 F j\pi_1(x)\cos\alpha, \quad (23)$$

$$\mathcal{L}_2^{\text{quad}} = \frac{1}{2}\partial_\mu\pi^a\partial^\mu\pi_a + \frac{1}{2}m_{12}[\pi_1(x)\partial_0\pi_2(x) - \pi_2(x)\partial_0\pi_1(x)] - \frac{1}{2}[m_1^2\pi_1^2(x) + m_2^2\pi_2^2(x) + m_3^2\pi_3^2(x)], \quad (24)$$

where, following the notation in [21], we have

$$m_{12} = 2\mu_I\cos\alpha, \quad (25)$$

$$m_1^2 = M^2\cos\alpha - (1 - a_1)\mu_I^2\cos(2\alpha) + 2B_0 j\sin\alpha, \quad (26)$$

$$m_2^2 = M^2\cos\alpha - (1 - a_1)\mu_I^2\cos^2\alpha + 2B_0 j\sin\alpha, \quad (27)$$

$$m_3^2 = M^2\cos\alpha + (1 - a_1)\mu_I^2\sin^2\alpha + 2B_0 j\sin\alpha. \quad (28)$$

Now, we follow the same steps as in [21] to obtain the pion dispersion relation in terms of the parameters $m_{12}, m_{1,2,3}^2$. Note that to leading order, we can replace $\alpha = \alpha_0^{(2)}$, which in particular cancels the contribution proportional to $\pi_1(x)$ in (23) so that such a linear Lagrangian becomes a total derivative in the condensed phase and vanishes in the normal phase. Therefore, at this order, the linear Lagrangian does not play any role for the dispersion relation or in the free energy density. As we will discuss in Sec. III C 3, this no longer holds when all the NLO corrections are properly accounted for, so that term will have to be included.

At this order, we then get for the dispersion relation of charged and neutral pions, respectively,

$$E_\pm^2(p) = p^2 + \frac{1}{2}(m_1^2 + m_2^2 + m_{12}^2) \pm \frac{1}{2}\sqrt{4p^2 m_{12}^2 + (m_1^2 + m_2^2 + m_{12}^2)^2 - 4m_1^2 m_2^2}, \quad (29)$$

$$E_0^2(p) = p^2 + m_3^2, \quad (30)$$

where $p \equiv |\vec{p}|$. Now, setting $\alpha = \alpha_0^{(2)}$ given in (22) and $p = 0$, we get then the dependence of the static pion masses on the isospin chemical potential, now including the correction from the a_1 term, which for $j = 0$ read

$$\begin{cases} M_\pm^2 = M^2 + (1 + a_1)\mu_I^2 \pm 2\mu_I\sqrt{M^2 + a_1\mu_I^2}, \\ M_0^2 = M^2, \end{cases} \quad \mu_I < \mu_c, \quad (31)$$

$$\begin{cases} M_+^2 = (1 - a_1)\mu_I^2 + \frac{3+a_1}{(1-a_1)^2}\frac{M^4}{\mu_I^2}, \\ M_-^2 = 0, \\ M_0^2 = (1 - a_1)\mu_I^2. \end{cases} \quad \mu_I > \mu_c, \quad (32)$$

In fact, from the previous analysis of the dispersion relation, we realize that the displacement of the critical point produced by the a_1 term can be understood as follows, consistent within the effective Lagrangian framework. The usual condition for BEC reads $\mu_c = \tilde{M}_-$ with $\tilde{M}_- = \tilde{E}_-(p = 0)$ and $\tilde{E}_-(p)$ the π^- particle mass and energy, respectively, below the critical point, for which the Bose-Einstein distribution diverges. In other words,

$M_-(\mu_c) = 0$ with $M_-(\mu_I) = \tilde{M} - \mu_I$. However, within the effective Lagrangian framework, one has μ_I-dependent interactions, which in particular enter in the particle dispersion relation and may then modify the critical point. This is the case for $a_1 \neq 0$, for which we expect the same modification in the charged pion mass as in the case of EM interactions. Actually, from (31), we see that the effect of the new a_1 term below μ_c amounts to the shift $M^2 \to M^2 + a_1\mu_I^2$, which we readily recognize as the same effect as the charged pion mass shift $M^2 \to M^2 + 2C\frac{e^2}{F^2}$ which takes place when EM interactions are included, coming from the term $\Delta\mathcal{L}_2^{\rm EM} = C\mathrm{Tr}(QUQU^\dagger)$ with Q the quark charge matrix [43–46]. The origin of that mass shift is in both cases the Lagrangian contribution breaking isospin only in the charged pion directions, so it does not affect the neutral pion mass. Therefore, from $M^2 + a_1\mu_c^2 = \mu_c^2$ we would readily have the shifted $\mu_c = M/\sqrt{1-a_1}$. Actually, one can check that $M_-(\mu_c) = 0$ with M_- in (31) for any a_1. Thus, as in the $a_1 = 0$ case, the vanishing mass of one of the charged pions signals the onset of BEC condensation as a Goldstone mode corresponding to the $U(1)_{I_3}$ spontaneous symmetry breaking of the vacuum in that phase, i.e., with a nonzero pion expectation value. The above mass dependence is plotted in Fig. 1 for a sample value of $a_1 = -0.1$ compared to the $a_1 = 0$ case, the qualitative dependence with μ_I being quite similar, although note that a_1 introduces a nonpolynomial dependence below μ_c.

From the free energy density in (21), we also get the quark and pion condensates, as well as the isospin density. Namely, from (18)–(20), we get, replacing $\alpha = \alpha_0$ and for $j = 0$,

$$\langle\bar{q}q\rangle^{(2)}(\mu_I) = \begin{cases} -2B_0F^2, & \mu_I < \mu_c, \\ \frac{-2B_0F^2M^2}{(1-a_1)\mu_I^2}, & \mu_I > \mu_c. \end{cases} \tag{33}$$

$$\langle i\bar{q}\gamma_5\tau_1 q\rangle^{(2)}(\mu_I) = \begin{cases} 0, & \mu_I < \mu_c, \\ -2B_0F^2\sqrt{1-\frac{M^4}{(1-a_1)^2\mu_I^4}}, & \mu_I > \mu_c, \end{cases} \tag{34}$$

$$n_I^{(2)}(\mu_I) = \begin{cases} \frac{1}{2}(a_1+a_2)F^2\mu_I, & \mu_I < \mu_c, \\ \frac{1}{2}F^2\mu_I\left(2 - a_1 + a_2 - \frac{2M^4}{(1-a_1)\mu_I^4}\right), & \mu_I > \mu_c. \end{cases} \tag{35}$$

Note that the only dependence with a_2 shows up in the pion density, which should remain zero below the BEC point. Therefore, with that physical requirement, we fix

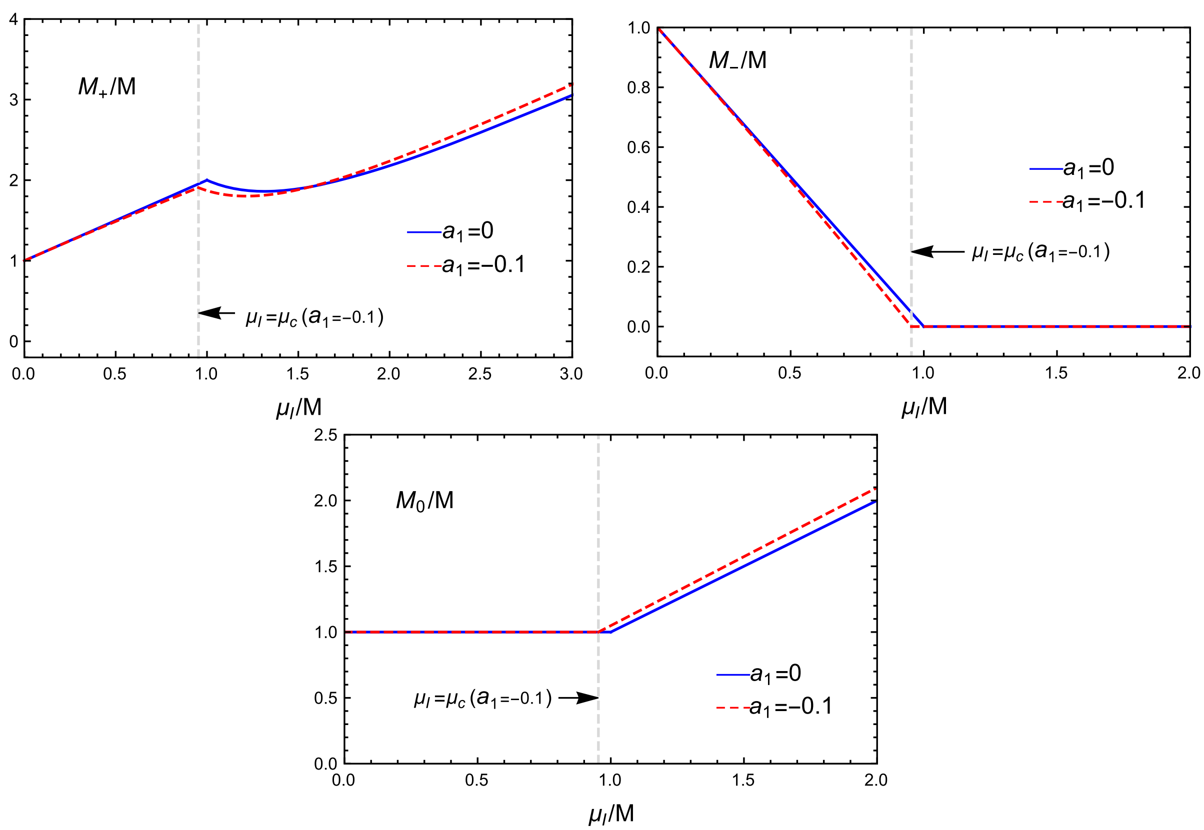

FIG. 1. Dependence of pion masses with isospin chemical potential to leading order in ChPT with and without the extra term, for a sample value $a_1 = -0.1$.

$$a_2 = -a_1 + \mathcal{O}(1/F^2) \tag{36}$$

up to higher-order corrections, which leaves us only with one free parameter at this order.

The condition (36) is an example of the physical conditions implying LEC relations mentioned in Sec. II. It has to be understood as a constraint on the $a_{1,2}$ relative size under the chiral power counting. As explained, this is not contradictory to the effective Lagrangian framework, where at the Lagrangian level the field operators corresponding to $a_{1,2}$ are indeed independent. In Sec. IV, we will discuss additional constraints at NLO. In fact, as already commented, we will see that when all contributions from ϵ_4 are properly taken into account, one gets actually $a_{1,2} = \mathcal{O}(1/F^2)$ so that all a_1 corrections to the free energy density fall formally into the NLO.

In turn, note that the coefficients in front of the two μ_I^2 terms in (10) are of opposite sign. This is a consequence of the covariant derivative structure $[Q,U][Q,U^\dagger]$ entering that term and leading in particular to $D_\mu \mathbb{1} = 0$ so that they do not contribute to the free energy density in the normal vacuum. Since the $a_{1,2}$ terms do not come from the covariant derivative, the condition (36) has to be fulfilled. An alternative way to understand the condition (36) is that only the difference of those two operators is allowed to leading order, as they actually appear in the μ_I^2 covariant derivative term in (10), and so on for the NLO operator combinations arising from the constraints that we will discuss in Sec. IV.

B. Comparison with lattice

Before proceeding to the ϵ_4 calculation, and in order to have a first and more quantitative idea of the effect of the new terms, we will compare the results in Sec. III A with those obtained in the lattice.

Using only the ϵ_2 results simplifies the analysis since the only undetermined constant is a_1, which we will fit here to the lattice points. This will allow us, on the one hand, to have a neater comparison with previous works [22] where the main contribution to the different observables comes from ϵ_2. On the other hand, it is important to discern whether $a_1 \neq 0$ is preferred for lattice results, since, in principle, as commented in the Introduction, lattice points are compatible with $\mu_c < M_\pi$, which would call for $a_1 < 0$ according to (22). In addition, as we are about to see, this analysis will support numerically the idea that the a_1 corrections are parametrically much smaller than the rest of the contributions coming from ϵ_2, which is confirmed by our analysis in Sec. IV, and which in particular implies that to LO, one still has formally $\mu_c = M$. Once we include properly all the ϵ_4 contributions, for the rest of undetermined constants arising from the $\mathcal{L}_4^Q$ Lagrangian in (15) we will consider natural values, as discussed below.

For that purpose, we will consider for the quark and pion condensates the recent lattice results provided in [22] at $T = 0$ coming from the collaboration [38]. The latter are given for a finite pionic source. We take $j = 0.00517054 M_\pi$, one of the two values considered in [22]. As for the isospin density, we compare with the results quoted in [38] for $j = 0$ and T small enough to provide an accurate enough description of the $T = 0$ case.

We also fix, as in [22,38],

$$\begin{aligned}
&M_\pi = 131\ \text{MeV}, \qquad M = 132.49\ \text{MeV},\\
&F_\pi = 90.51\ \text{MeV}, \qquad F = 84.93\ \text{MeV},\\
&m = 3.47\ \text{MeV}, \qquad B_0 = 2529.34\ \text{MeV},
\end{aligned} \tag{37}$$

where, for the sake of comparison with the lattice, we have used their physical M_π, F_π values, which using the one-loop standard ChPT expressions [41], give rise to the values of the tree-level M, F quoted in (37). In addition, we assign a characteristic uncertainty of 5% to the lattice data, following again [22,38]. Thus, we show here the results of three different fits, which are summarized in Table I and Figs. 2–4. The uncertainty bands in the figures and the uncertainty range for the a_1 parameter correspond to the 95% confidence level.

Those results lead to the following partial conclusions. First, the quark and pion condensates can be reasonably fitted with $a_1 = 0$ within the uncertainties considered (fit 1). Fitting only the quark (pion) condensate favors a positive (negative) a_1 value, still compatible with zero. However, the conclusion is very different when fitting the isospin density in fit 2, for which we have included only the lattice points with $\mu_I > M_\pi$. As explained in [38], the lattice uncertainty for $\mu_I \sim M_\pi$ is actually much higher, although we have still plotted the first lattice point below μ_I and given in [38]. Note that such a point lies below M_π with a nonzero isospin density central value, which is actually favored by our present analysis with negative a_1. In fact, as can be seen from the results in Table I, the lattice results for n_I are much better fitted with a negative value for a_1 than for $a_1 = 0$, as the values of the corresponding $\chi^2/\text{d.o.f.}$ clearly show. The same conclusion is reached when performing a combined fit of the three observables (fit 3). Note also that fits 2 and 3 for n_I reproduce quite well the two ends of the lattice points, i.e., the closest points to

TABLE I. Results for the a_1 constant in different fits to quark and pion condensates and isospin density.

Fit	a_1	$\chi^2/\text{d.o.f.}$	$\chi^2/\text{d.o.f.}$, $a_1 = 0$
1: $\langle i\bar{q}\gamma_5\tau_1 q\rangle$, $\langle\bar{q}q\rangle$	$0.000^{+0.036}_{-0.038}$	0.64	0.64
2: n_I	-0.020 ± 0.007	1.39	7.30
3: $\langle i\bar{q}\gamma_5\tau_1 q\rangle$, $\langle\bar{q}q\rangle$, n_I	-0.019 ± 0.007	0.84	2.03

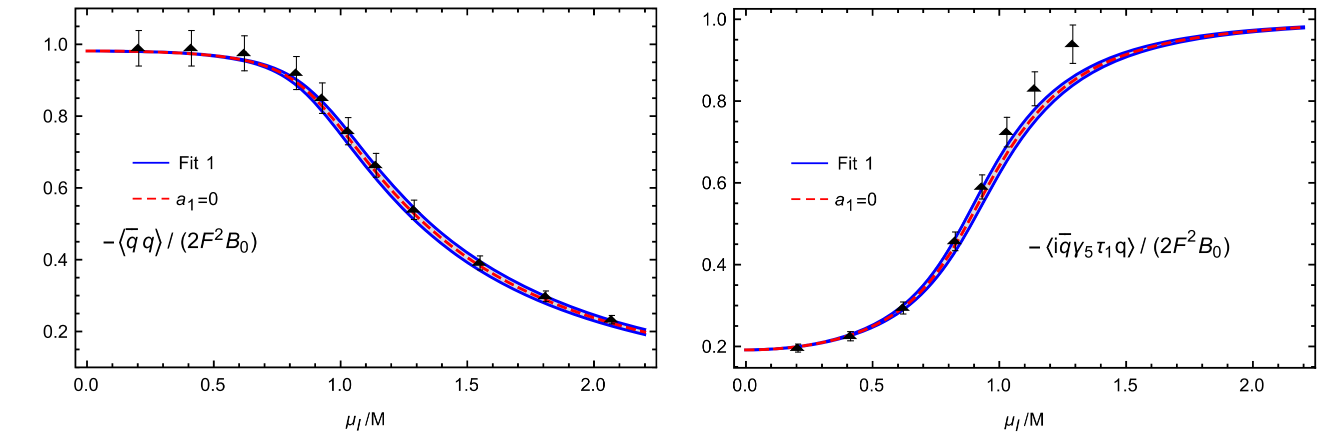

FIG. 2. Combined fit of the quark condensate (left) and the pion condensate (right) for $j = 0.00517054 M_\pi$. Lattice points are taken from [22].

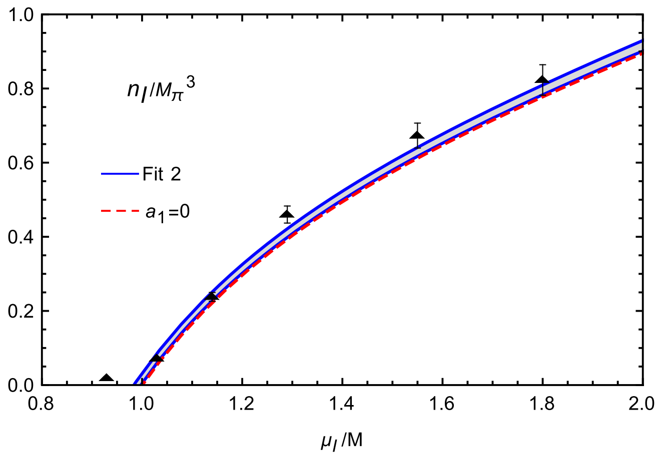

FIG. 3. Fit of the isospin density for $j = 0$. Lattice points are taken from [38].

$\mu_I = M_\pi$ and those for larger $\mu_I > M_\pi$, improving over the $a_1 = 0$ case. As for the numerical value of a_1 obtained in the fits, we confirm what we had already advanced, i.e., $|a_1| \ll 1$, which supports the idea that a_1 should be parametrically included in the NLO corrections, as we will formally prove in Sec. IV.

To end this section, we show the results for $\alpha_0^{(2)}$ (Fig. 5), i.e., the solution of the equation $\frac{\partial \epsilon_2}{\partial \alpha} = 0$, for the value of a_1 obtained in the joint fit 3, both for $j = 0$ and for the value of j used here. The explicit expression of $\alpha_0^{(2)}$ is given in (22). While for $j = 0$, the a_1 contribution changes the transition point, as already commented, for $j \neq 0$ the transition is a crossover, and a_1 merely modifies the inflection point of the $\alpha_0^{(2)}$ function.

To summarize this section, lattice results are compatible with $a_1 < 0$ and parametrically small, improving the description of the isospin density and the overall description of n_I and the two condensates.

C. Fourth-order contributions

The next-to-leading corrections ϵ_4 to the free energy density come from three different sources, which we will analyze separately below.

(i) Loop corrections coming from the quadratic field terms (24) in the $\mathcal{L}_2$ Lagrangian, which can be obtained in a similar fashion to the standard free-field contributions to the partition function in vacuum, including now the μ_I corrections to the pion dispersion relation [21].

(ii) The constant terms coming from the $\mathcal{L}_4$ Lagrangian in (14) and (15). The LEC coming from this contribution, including the new ones coming from $\mathcal{L}_4^Q$, will be renormalized to absorb the loop divergences.

(iii) The linear-field terms coming from $\mathcal{L}_2$ and given in (23) will also contribute as long as the minimizing angle $\alpha_0^{\mathrm{NLO}} \neq \alpha_0^{(2)}$. This contribution has not been considered in previous works on this subject and is discussed below.

1. Loop contributions

Following the same steps as in previous works [21], we can write the one-loop contribution to the free energy density as

$$\epsilon_4^{\mathrm{loop}} = \frac{1}{2}\int_p [E_+(p) + E_-(p)] + \frac{1}{2}\int_p E_0(p) \qquad (38)$$

with $E_\pm(p)$ and $E_0(p)$ in (29) and (30) and, following the notation in [21],

$$\int_p = \mu^{2\epsilon} \int \frac{d^{D-1}p}{(2\pi)^{D-1}} \qquad (39)$$

with $D = 4 - 2\epsilon$ and $\epsilon \to 0^+$ and μ the dimensional regularization (DR) scale.

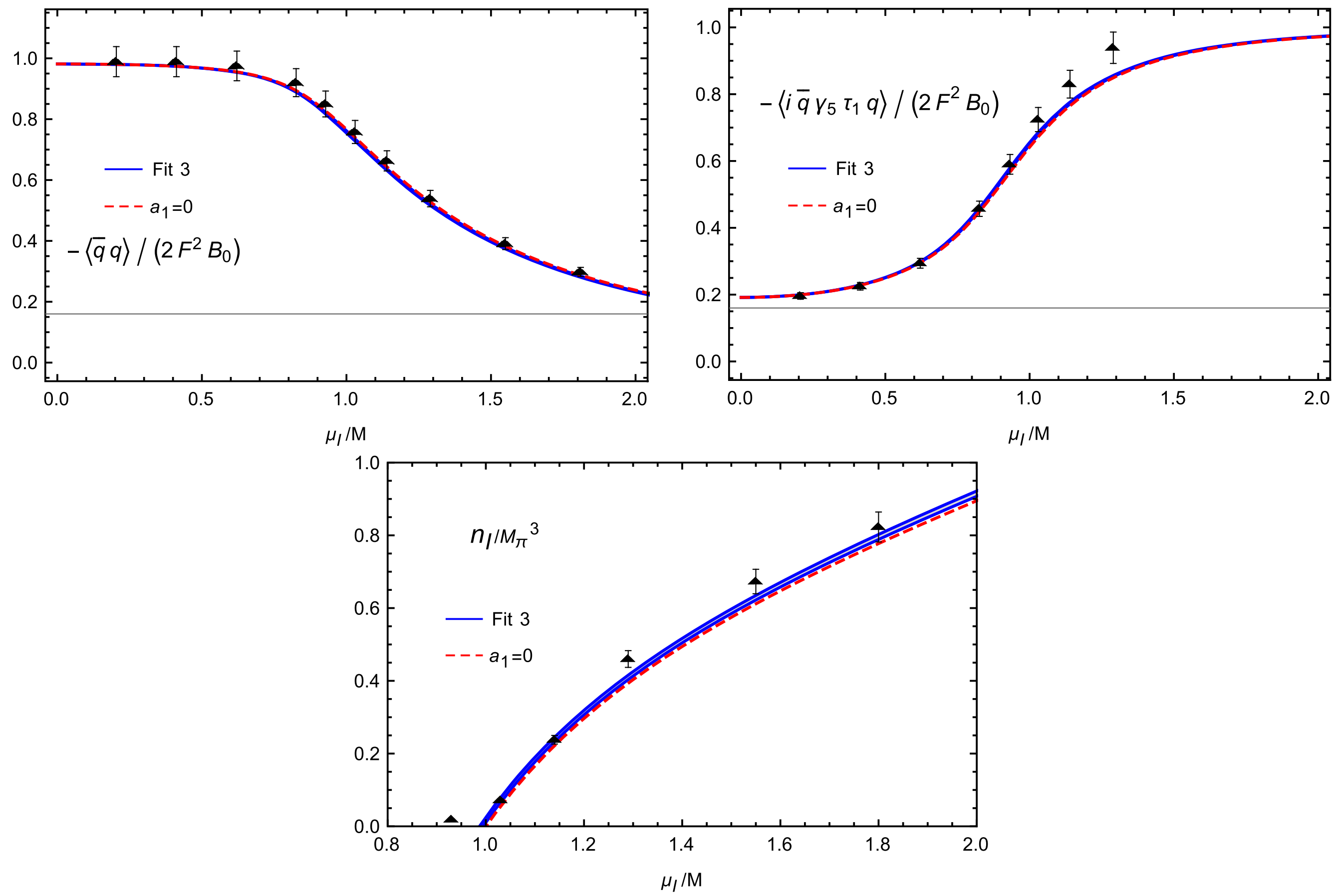

FIG. 4. Combined fit of the quark condensate (upper left panel), the pion condensate (upper right panel), and the isospin density (lower panel). Lattice points are the same as in Figs. 2 and 3.

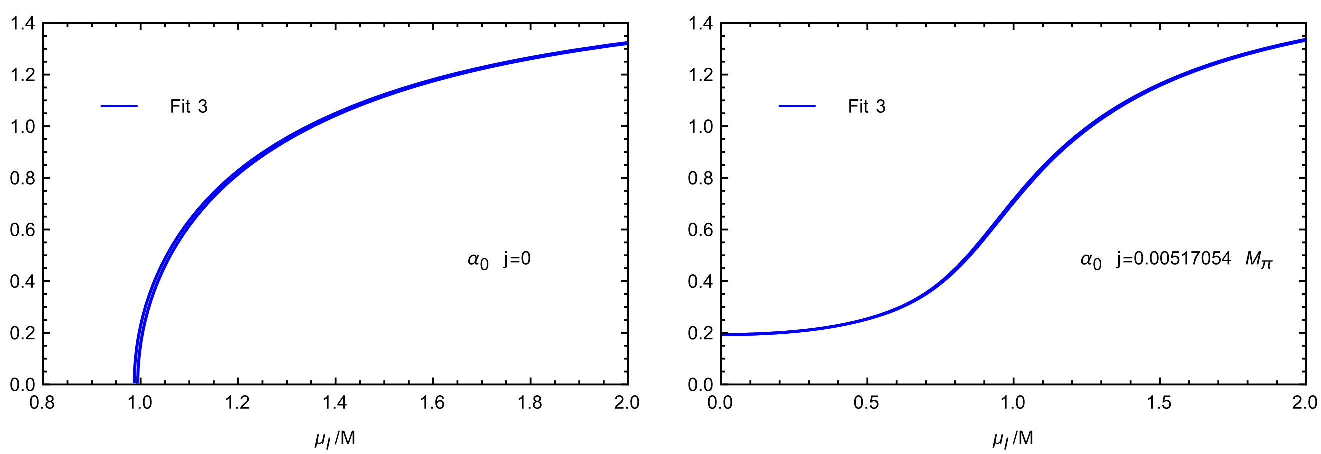

FIG. 5. $\alpha_0^{(2)}$ as a function of μ_I/M for $j = 0$ (left) and $j = 0.00517054 M_\pi$ (right).

The treatment of the above integrals separating their UV divergent contribution in DR follows the same steps as in [21] except for the modifications proportional to a_1 in Eqs. (25)–(28). The contribution from the charged pions to the one-loop free energy density can be written as

$$\frac{1}{2}\int_p [E_+(p) + E_-(p)] = \epsilon_{4,+-}^{\rm div} + \epsilon_{4,+-}^{\rm fin} \tag{40}$$

with

$$\epsilon_{4,+-}^{\rm div} = \frac{1}{2}\int_p [E_1(p) + E_2(p)], \tag{41}$$

$$\epsilon_{4,+-}^{\rm fin} = \frac{1}{2}\int_p [E_+(p) + E_-(p) - E_1(p) - E_2(p)], \qquad (42)$$

and where we have introduced the quantities $E_{1,2}(p)$ given by

$$\begin{aligned} E_{1,2}(p) &= \sqrt{p^2 + \hat{m}_{1,2}^2}, \\ \hat{m}_1^2 &= (M^2 + \mu_I^2\cos\alpha)\cos\alpha - (1-a_1)\mu_I^2\cos 2\alpha \\ &\quad + 2B_0 j\sin\alpha, \\ \hat{m}_2^2 &= (M^2 + a_1\mu_I^2\cos\alpha)\cos\alpha + 2B_0 j\sin\alpha, \\ \hat{m}_3^2 &= m_3^2 = M^2\cos\alpha + (1-a_1)\mu_I^2\sin^2\alpha + 2B_0 j\sin\alpha. \end{aligned} \qquad (43)$$

Separating in this way the divergent part of the charged contribution, $\epsilon_{4,+-}^{\rm div}$ in (41) has the form of the neutral part in (38) and is easier to handle in DR. Actually, note that the large-p behavior of $E_1 + E_2$ is the same as the sum $E_+ + E_-$. The finite contribution (subtraction integral) $\epsilon_{4,+-}^{\rm fin}$ can be calculated numerically. Thus, in DR we get for the full divergent part

$$\begin{aligned} (\epsilon_4^{\rm loop})_{\rm div} &= \frac{1}{2}\int_p [E_1(p) + E_2(p)] + \frac{1}{2}\int_p E_0(p) \\ &= -\sum_{i=1}^{3}\frac{\hat{m}_i^4}{4(4\pi)^2}\left[N_\epsilon + \frac{3}{2} + \log\left(\frac{\mu^2}{\hat{m}_i^2}\right)\right] \end{aligned} \qquad (44)$$

with $N_\epsilon = \frac{1}{\epsilon} - \gamma + \log(4\pi)$ and γ the Euler constant.

2. $\mathcal{O}(p^4)$ Lagrangian and renormalization

The contributions to the free energy density coming from the constant part in the $\mathcal{O}(p^4)$ Lagrangian (14) and (15) are, respectively, given by

$$\begin{aligned} \epsilon_4^{40} &= -(l_1 - l_2)\mu_I^4\sin^4\alpha - l_4 M^2\mu_I^2\cos\alpha + l_4 M^2\mu_I^2\cos^3\alpha \\ &\quad - 2l_4 B_0\mu_I^2 j\sin\alpha + 2l_4 B_0\mu_I^2 j\sin\alpha\cos^2\alpha \\ &\quad - (h_1 - l_4)M^4 - (l_3 + l_4)M^4\cos^2\alpha \\ &\quad - 2B_0 j(l_3 + l_4)M^2\sin(2\alpha) \\ &\quad - 4B_0^2 j^2[h_1 - l_4 + (l_3 + l_4)\sin^2\alpha], \end{aligned} \qquad (45)$$

$$\begin{aligned} \epsilon_4^{4Q} &= -\hat{q}_1\mu_I^4\sin^4\alpha - \frac{1}{2}\hat{q}_2 M^2\mu_I^2\cos\alpha - \frac{1}{2}\hat{q}_3 M^2\mu_I^2\cos^3\alpha \\ &\quad - \hat{q}_4 B_0\mu_I^2 j\sin\alpha - \hat{q}_5 B_0\mu_I^2 j\sin\alpha\cos^2\alpha \\ &\quad - \hat{q}_6\mu_I^4\cos^2\alpha - \hat{q}_7\mu_I^4 \end{aligned} \qquad (46)$$

with

$$\begin{aligned} \hat{q}_1 &= q_{10} - 2q_2 - 2q_3 - q_4, & \hat{q}_5 &= 8(q_6 + q_7), \\ \hat{q}_2 &= 4q_5 - 2q_6 - 8q_7, & \hat{q}_6 &= \frac{1}{2}(-2q_1 + 2q_{10} - 2q_2 + q_9), \\ \hat{q}_3 &= 4(q_6 + 2q_7), & \hat{q}_7 &= \frac{1}{4}(4q_1 - 3q_{10} + 4q_2 + q_8 - q_9), \\ \hat{q}_4 &= 4(q_5 - q_6). \end{aligned}$$

Comparing (46) with (45), we see that new terms introduce μ_I-dependent corrections as follows: $\hat{q}_1$ shifts the $(l_1 - l_2)\mu_I^4$ contribution, $\hat{q}_{2,3,4,5}$ modify, respectively, the four $l_4\mu_I^2$ terms, whereas $\hat{q}_{6,7}$ introduce new μ_I^6 terms. Of those new seven independent LECs appearing in the free energy density, $\hat{q}_4$ and $\hat{q}_5$ will not contribute for $j = 0$, and the $\hat{q}_7$ term is independent of α, so it does not contribute to the free energy density minimum.

The new LECs will precisely absorb the new loop divergences dependent on a_1 included in (44). Thus, the renormalized free energy density at NLO resulting from adding all the contributions mentioned before can be written as

$$\begin{aligned}\epsilon_4^{\rm loop}+\epsilon_4^{40}+\epsilon_4^{4Q}=&-\frac{1}{(4\pi)^2}\left[\frac{3}{2}-\bar{l}_3+4\bar{l}_4+\log\left(\frac{M^2}{\hat{m}_2^2}\right)+2\log\left(\frac{M^2}{\hat{m}_3^2}\right)\right]\left[\frac{1}{4}M^4\cos^2\alpha+B_0^2j^2\sin^2\alpha+\frac{1}{2}M^2B_0j\sin(2\alpha)\right]\\
&-\frac{1}{2(4\pi)^2}\left\{\frac{1}{2}+\frac{1}{3}\bar{l}_1+\frac{2}{3}\bar{l}_2+2(4\pi)^2\hat{q}_1^r-\frac{a_1}{2}\left[3(1-a_1)+4(1-a_1)\log\left(\frac{\mu^2}{\hat{m}_1^2}\right)-a_1\log\left(\frac{\mu^2}{\hat{m}_2^2}\right)\right.\right.\\
&\left.\left.+(2-a_1)\log\left(\frac{\mu^2}{m_3^2}\right)\right]+\log\left(\frac{M^2}{m_3^2}\right)\right\}\mu_I^4\sin^4\alpha-\frac{1}{(4\pi)^2}\left\{\frac{1}{2}+\bar{l}_4+\frac{(4\pi)^2}{2}\hat{q}_2^r-\frac{a_1}{2}\left[1+\log\left(\frac{\mu^2}{\hat{m}_1^2}\right)\right.\right.\\
&\left.\left.+\log\left(\frac{\mu^2}{m_3^2}\right)\right]+\log\left(\frac{M^2}{m_3^2}\right)\right\}M^2\mu_I^2\cos\alpha+\frac{1}{(4\pi)^2}\left\{\frac{1}{2}+\bar{l}_4-\frac{(4\pi)^2}{2}\hat{q}_3^r-\frac{a_1}{2}\left[2+2\log\left(\frac{\mu^2}{\hat{m}_1^2}\right)\right.\right.\\
&\left.\left.+\log\left(\frac{\mu^2}{\hat{m}_2^2}\right)+\log\left(\frac{\mu^2}{m_3^2}\right)\right]+\log\left(\frac{M^2}{m_3^2}\right)\right\}M^2\mu_I^2\cos^3\alpha-\frac{2}{(4\pi)^2}\left\{\frac{1}{2}+\bar{l}_4+\frac{(4\pi)^2}{2}\hat{q}_4^r\right.\\
&\left.-\frac{a_1}{2}\left[1+\log\left(\frac{\mu^2}{\hat{m}_1^2}\right)+\log\left(\frac{\mu^2}{m_3^2}\right)\right]+\log\left(\frac{M^2}{m_3^2}\right)\right\}B_0j\mu_I^2\sin\alpha+\frac{2}{(4\pi)^2}\left\{\frac{1}{2}+\bar{l}_4-\frac{(4\pi)^2}{2}\hat{q}_5^r\right.\\
&\left.-\frac{a_1}{2}\left[2+2\log\left(\frac{\mu^2}{\hat{m}_1^2}\right)+\log\left(\frac{\mu^2}{\hat{m}_2^2}\right)+\log\left(\frac{\mu^2}{m_3^2}\right)\right]+\log\left(\frac{M^2}{m_3^2}\right)\right\}B_0j\mu_I^2\sin\alpha\cos^2\alpha\\
&-\frac{1}{2(4\pi)^2}\left\{2(4\pi)^2\hat{q}_6^r-\frac{a_1}{2}\left[1-3a_1+2(1-2a_1)\log\left(\frac{\mu^2}{\hat{m}_1^2}\right)-2a_1\log\left(\frac{\mu^2}{\hat{m}_2^2}\right)\right]\right\}\mu_I^4\cos^2\alpha\\
&-\frac{1}{2(4\pi)^2}\left\{2(4\pi)^2\hat{q}_7^r+\frac{a_1}{2}\left[1-2a_1+(2-3a_1)\log\left(\frac{\mu^2}{\hat{m}_1^2}\right)-a_1\log\left(\frac{\mu^2}{\hat{m}_2^2}\right)\right]\right\}\mu_I^4\\
&-\frac{1}{(4\pi)^2}(\bar{h}_1-\bar{l}_4)[M^2+4B_0^2j^2]+\epsilon_{4,+-}^{\rm fin},\end{aligned}\tag{47}$$

where the renormalized and scale-independent $\bar{l}_i, \bar{h}_i$ are the standard ones given in [22,41], while the new LECs are renormalized as

$$\hat{q}_i=\hat{q}_i^r(\mu)-\eta_i\frac{\mu^{-2\epsilon}}{2(4\pi)^2}[N_\epsilon+1]\tag{48}$$

with

$$\begin{aligned}&\eta_1=-3a_1+3a_1^2, && \eta_5=8a_1,\\ &\eta_2=-4a_1, && \eta_6=-a_1+3a_1^2,\\ &\eta_3=8a_1, && \eta_7=a_1-2a_1^2,\\ &\eta_4=-4a_1,\end{aligned}\tag{49}$$

where, as usual, the μ dependence of the renormalized LECs cancels with that of the loops, rendering the free energy density finite and scale independent. In the following sections, we will analyze the effect of these new LECs on the μ_I dependence of the different observables obtained from the free energy density.

The numerical values we will use for the $\bar{l}_i$ will be the same as the previous works on this subject [22,39] for an easier comparison. Thus, we will take the central values of the $\bar{l}_i, \bar{h}_i$ from [49]:

$$\begin{aligned}&\bar{l}_1=-0.4, && \bar{l}_2=4.3, && \bar{l}_3=2.9,\\ &\bar{l}_4=4.4, && \bar{h}_1-\bar{l}_4=-1.5,\end{aligned}\tag{50}$$

which have been used to study the quark and pion condensates in [22] and the isospin density in [39] at zero temperature.

Recall that the $\bar{l}_i, \bar{h}_i$, although scale independent are mass dependent, and therefore, there might be slight numerical variations from the values (50) when taking the masses in (37). Those variations are logarithmic and therefore numerically negligible, so for our purposes of comparing with previous works, we will still use the values in (50).

As for the $\hat{q}_i$ constants, for simplicity we will consider them within natural values defined from a characteristic ChPT uncertainty range [45,46] as

$$|\hat{q}_i^r|\leq\frac{1}{16\pi^2}\tag{51}$$

at a typical chiral scale, which we will set as $\mu=M_\rho\simeq$ 770 MeV from now on. Recall that all our results are independent of the scale μ.

3. Linear terms

The solution for the angle minimizing ϵ_2 given in (22) for $j=0$ is such that the linear term in (23) proportional to $\pi_1(x)$ vanishes, so the linear terms can be ignored since the derivative term in (23) does not contribute to ϵ_2. However, this is not necessarily true to higher orders. Thus, let us consider values of α perturbatively close to $\alpha_0^{(2)}$, around which the minimum of $\epsilon_2 + \epsilon_4$ will be, i.e.,

$$\alpha = \alpha_0^{(2)} + \delta\alpha_0 \tag{52}$$

with $\alpha_0^{(2)} = \mathcal{O}(1)$, $\delta\alpha_0 = \mathcal{O}(1/F)$ in the chiral expansion, Then we can write

$$\mathcal{L}_2^{\text{lin}} = f'(\alpha_0^{(2)})(\alpha - \alpha_0^{(2)})\pi_1(x) + \mathcal{O}(1/F) + \ldots, \tag{53}$$

where the dots denote derivative terms and, according to (23),

$$f(\alpha) = -F\sin\alpha[M^2 - (1-a_1)\mu_I^2\cos\alpha] + 2B_0 F j\cos\alpha. \tag{54}$$

The above linear contribution to NLO can be reabsorbed into a redefinition of the π_1 field, over which we are integrating to get the free energy density. Namely,

$$\pi_1 \to \pi_1 + \frac{f'(\alpha_0^{(2)})}{m_1^2(\alpha_0^{(2)})}(\alpha - \alpha_0^{(2)}). \tag{55}$$

The above shift eliminates the linear term at this order and completing squares generates the following additional $\mathcal{O}(1)$ perturbative contribution to the NLO free energy density:

$$\epsilon_4^{\text{lin}} = -\frac{1}{2}\frac{[f'(\alpha_0^{(2)})]^2}{m_1^2(\alpha_0^{(2)})}(\alpha - \alpha_0^{(2)})^2 \tag{56}$$

with m_1^2 in (26). The contribution (56) has to be added to those in (47) to get the full ϵ_4. Minimizing now $\epsilon_2 + \epsilon_4$ with respect to α will give rise to the new minimum, which we denote α_0^{NLO} lying perturbatively around $\alpha_0^{(2)}$. Note that the linear contribution (56) arises even for $a_1 = 0$, its contribution to the different observables being

$$\Delta\langle\bar{q}q\rangle_{\text{lin}}^{\text{NLO}} = \frac{\partial\epsilon_4^{\text{lin}}}{\partial m} = -B_0F^2\cos(\alpha_0^{(2)})(\alpha - \alpha_0^{(2)})^2, \tag{57}$$

$$\Delta\langle i\bar{q}\gamma_5\tau_1 q\rangle_{\text{lin}}^{\text{NLO}} = \frac{\partial\epsilon_4^{\text{lin}}}{\partial j} = -B_0F^2\sin(\alpha_0^{(2)})(\alpha - \alpha_0^{(2)})^2, \tag{58}$$

$$\Delta(n_I)_{\text{lin}}^{\text{NLO}} = -\frac{\partial\epsilon_4^{\text{lin}}}{\partial\mu_I} = -\mu_I F^2(1-a_1)\cos(2\alpha_0^{(2)})(\alpha - \alpha_0^{(2)})^2. \tag{59}$$

To have a more quantitative idea of the effect of this correction, we have plotted in Fig. 6 the result for the minimizing angle α_0, comparing $\alpha_0^{(2)}$ with α_0^{NLO}, with and without including the linear term contribution (56). For easier comparison with previous works, we have not included in that plot the new contributions coming from the a_1 and $\hat{q}_i$ terms. We consider both the $j = 0$ and $j \neq 0$ situations. As we can see in that figure, the inclusion of the linear term may generate sizable differences between the NLO and LO results. Actually, for some values of the constants involved, those linear corrections can be such that the effective potential stops having a minimum above a certain μ_I value. We can actually see this behavior in the plot shown in Fig. 6 for which that limiting value is $\mu_I \simeq$ 300 MeV for $j = 0$ and $\mu_I \simeq 340$ MeV for the $j \neq 0$ value considered. The deviations with respect to the LO indicate that we are reaching the borderline of the ChPT validity limit where, in particular, the very same approximation followed in (52) and (53) would fail. This is actually consistent with lattice analyses showing that deviations from ChPT around those μ_I values signal the onset of the BCS phase [25]. Nevertheless, it should be taken into

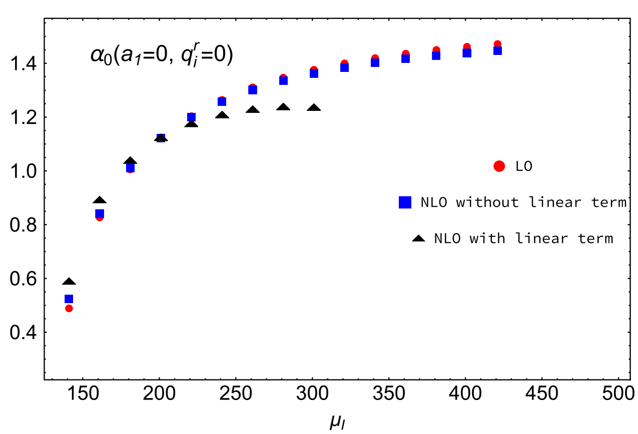

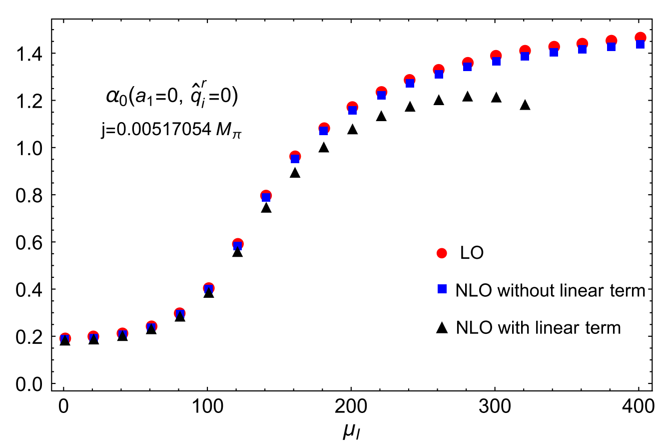

FIG. 6. Effect of the linear term in the minimizing angle α_0 for $j = 0$ (left) and $j \neq 0$ (right). The LO here refers to $\alpha_0^{(2)}$ in (22).

account that the actual value of such a validity limit depends also on the rest of the LEC involved, as we will discuss in detail below.

IV. PHYSICAL CONSTRAINTS

A. Constraints on the LEC from the isospin density

First, let us discuss the constraints arising from the condition of vanishing isospin density for $\mu_I < \mu_c$ and $j = 0$, i.e., the extension of the constraint (36) to include the NLO $\mathcal{O}(1/F^2)$ corrections. Let us denote $\mu_c^{(2)} = \frac{M}{\sqrt{1-a_1}}$ and $\mu_c^{\rm NLO}$ the NLO value for μ_c which will be determined in Sec. IV B below and which depends on the $\hat{q}_i^r$ constants. We obtain the isospin density below $\mu_c^{\rm NLO}$ by taking the derivative of $\epsilon_2 + \epsilon_4$ with respect to μ_I and setting $j = \alpha = 0$ [note that by definition, $\alpha_0^{\rm NLO}(\mu_I < \mu_c^{\rm NLO}) = 0$]. In doing so, we must be careful with the linear contribution (56). Such a contribution vanishes for $\alpha = 0$ and $\mu_I < \mu_c^{(2)} = \frac{M}{\sqrt{1-a_1}}$ since $\alpha_0^{(2)}(\mu_I < \mu_c^{(2)}) = 0$. However, it would contribute for $\mu_c^{(2)} < \mu_I < \mu_c^{\rm NLO}$ if $\mu_c^{(2)} < \mu_c^{\rm NLO}$. Thus, we get

(i) If $\mu_c^{(2)} > \mu_c^{\rm NLO} \Rightarrow n_I(\mu_I < \mu_c^{\rm NLO}) = n_0(\mu_I)$

(ii) If

$$\mu_c^{(2)} < \mu_c^{\rm NLO} \Rightarrow n_I(\mu_I < \mu_c^{\rm NLO}) = \begin{cases} n_0(\mu_I) + n_1(\mu_I) & \mu_c^{(2)} < \mu_I < \mu_c^{\rm NLO}, \\ n_0(\mu_I) m & \mu_I < \mu_c^{(2)} \end{cases}$$

with

$$\begin{aligned} n_0(\mu_I) &= \frac{F^2}{2}(a_1+a_2)\mu_I + M^2(\hat{q}_2^r + \hat{q}_3^r)\mu_I + 4(\hat{q}_6^r + \hat{q}_7^r)\mu_I^3 + \frac{a_1}{8\pi^2(M^2 + a_1\mu_I^2)} \\ &\quad \times \left[\frac{M^4}{4}\mu_I + (M^2 + a_1\mu_I^2)^2 \log\left(\frac{\mu^2}{M^2 + a_1\mu_I^2}\right)\right] + \mathcal{O}\left(\frac{1}{F^2}\right), \\ n_1(\mu_I) &= \frac{1}{2}\frac{\partial}{\partial\mu_I}\left[\frac{\alpha_0^{(2)}(\mu_I) f_0{}'[\alpha_0^{(2)}(\mu_I)]}{m_1(\mu_I)}\right]^2 + \mathcal{O}\left(\frac{1}{F^2}\right), \end{aligned} \tag{60}$$

where f_0 stands for the function f in (54) for $j = 0$, and we have followed [21] for the calculation of the loop integrals. Thus, since the μ_I dependence of the n_1 function above (coming from the linear term) is nonpolynomical, the only way to ensure that n_I vanishes for all μ_I below $\mu_c^{\rm NLO}$ is that the $\hat{q}_i^r$ satisfy the constraint

$$\mu_c^{\rm NLO}(\hat{q}_i^r) < \mu_c^{(2)}. \tag{61}$$

On the other hand, the condition that the n_0 function in (60) vanishes at this order, together with (36), implies the following additional constraints:

$$a_1, a_2 = \mathcal{O}\left(\frac{1}{F^2}\right), \tag{62}$$

$$a_1 + a_2 = -\frac{2M^2}{F^2}[\hat{q}_2^r(\mu) + \hat{q}_3^r(\mu)] + \mathcal{O}\left(\frac{1}{F^4}\right), \tag{63}$$

$$\hat{q}_6^r(\mu) + \hat{q}_7^r(\mu) = \mathcal{O}\left(\frac{1}{F^2}\right). \tag{64}$$

We remark that the condition (62) is fully consistent with having obtained a numerical value $|a_1| \ll 1$ in our fit study in Sec. III B. The situation is similar to the EM corrections in ChPT, where there are operators which are formally $\mathcal{O}(p^2)$, such as (3), but multiplied by e^2 which is a numerically small parameter. Actually, in view of the above considerations, if we had normalized $a_{1,2} = \frac{M^2}{F^2}\hat{a}_{1,2}$ so that the $\hat{a}_i$ would be parametrically of the same order as the $\hat{q}_i$, then conditions such as (63) or (69) below would translate into mass-independent relations. As commented in Sec. II, we are following the standard convention of ordering the Lagrangians according to the chiral order of the field operators, but from the above results, we could have equivalently considered formally the $a_{1,2}$ terms as part of the $\mathcal{O}(p^4)$ Lagrangian. On the other hand, Eq. (63) provides the explicit expression for the $\mathcal{O}(1/F^2)$ corrections in (36) and allows us to eliminate the dependence on a_2, while the condition (64) will be applied in what follows to eliminate the dependence on $\hat{q}_7^r$.

B. The critical BEC value at NLO

Once all the contributions to the free energy density $\epsilon_2 + \epsilon_4$ have been considered, the critical value $\mu_c^{\rm NLO}$ can be determined as the value for which $\alpha = 0$ flips from a local minimum to a local maximum, since $\frac{\partial\epsilon^{\rm NLO}}{\partial\alpha}|_{\alpha=0} = 0$. Therefore, expanding the free energy density around $\alpha = 0$,

$$\epsilon_2 + \epsilon_4 = \beta_0(\mu_I) + \beta_2(\mu_I)\alpha^2 + \mathcal{O}(\alpha^4), \tag{65}$$

we have

$$\beta_2(\mu_I)|_{\mu_I=\mu_c^{\rm NLO}} = 0. \tag{66}$$

From the free energy density calculated above, we find

$$\begin{aligned}\beta_2(\mu_I) &= \frac{1}{2}F_\pi^2[M_\pi^2-(1-a_1)\mu_I^2] \\ &\quad + \frac{1}{4}\mu_I^2[M^2(\hat{q}_2^r+3\hat{q}_3^r)+4\hat{q}_6^r\mu_I^2] \\ &\quad - \frac{F^2(\mu_I^4-M^4)}{2\mu_I^2} + \mathcal{O}\left(\frac{1}{F^2}\right),\end{aligned} \tag{67}$$

where M_π and F_π are the NLO ChPT pion decay constant and mass, respectively, [41] and where we have made use of the condition (62) so that the a_1 dependence in the NLO has been ignored. The last term in (67), proportional to F^2, comes from the linear-field contribution (56). Note that we are interested in the expansion around $\alpha = 0$ only in order to determine $\mu_c^{\rm NLO}$. Therefore, μ_I lies around $\mu_c^{(2)} = M[1+\mathcal{O}(F^{-2})]$ so that the linear-field contribution just mentioned remains of NLO, as it should.

From the previous expression, we see that only $\hat{q}_{2,3,6}^r$ and a_1 modify the critical BEC value. We show in Table II the value of $\mu_c^{\rm NLO}$ expected within the range of natural values for those constants in (51) and taking $a_1 = -0.019$, the central value of fit 3 to lattice results in Sec. III B. In addition, we have highlighted in the table the values for which the condition (61) holds. As explained, $\hat{q}_i^r$ values not satisfying that condition are not acceptable, since they give rise to a nonzero isospin density below the critical value. Note that, as happened in the $\mathcal{O}(p^2)$ analysis in Secs. III A and III C, our results support $\mu_c < M_\pi$, which, as shown in Sec. III B, is compatible with lattice results.

Anyhow, we remark that, due to the condition (62), parametrically we have at leading order

$$\mu_c^{LO} = M + \mathcal{O}\left(\frac{1}{F^2}\right) = M_\pi + \mathcal{O}\left(\frac{1}{F^2}\right), \tag{68}$$

while at next-to-leading order, from (67), the condition $\mu_c = M_\pi$ could be satisfied by imposing an additional constraint relating $\hat{q}_{2,3,6}^r$ and a_1, namely,

TABLE II. Critical value of the BEC transition for natural values of $\hat{q}_2^r$, $\hat{q}_3^r$, and $\hat{q}_6^r$. The highlighted values are those fulfilling the condition (61).

	$\hat{q}_6^r = \frac{1}{16\pi^2}$		$\hat{q}_6^r = -\frac{1}{16\pi^2}$	
$\mu_c^{\rm NLO}/M_\pi$	$\hat{q}_3^r = \frac{1}{16\pi^2}$	$\hat{q}_3^r = -\frac{1}{16\pi^2}$	$\hat{q}_3^r = \frac{1}{16\pi^2}$	$\hat{q}_3^r = -\frac{1}{16\pi^2}$
$\hat{q}_2^r = \frac{1}{16\pi^2}$	1.007	**0.935**	**0.916**	**0.803**
$\hat{q}_2^r = -\frac{1}{16\pi^2}$	1.005	**0.873**	**0.874**	**0.773**

$$\begin{aligned}\mu_c^{\rm NLO} = M_\pi \Rightarrow a_1F_\pi^2 + \frac{M_\pi^2}{2}\left[\hat{q}_2^r+3\hat{q}_3^r+4\hat{q}_6^r+\frac{\bar{l}_3}{8\pi^2}\right] \\ = \mathcal{O}\left(\frac{1}{F^2}\right),\end{aligned} \tag{69}$$

where $\bar{l}_3$ arises from the $M_\pi^2 - M^2$ difference [41], and we have replaced M by M_π in the NLO when the difference is of higher order. Since $M_\pi < M$, the consistency condition in Eq. (61) is compatible with (69), ensuring a vanishing isospin density below μ_c. If the constraint (69) is imposed, a further LEC could be eliminated.

It is important to observe from (69) that maintaining $\mu_c^{\rm NLO} = M_\pi$ requires at least one nonzero value for the new LEC $a_1, \hat{q}_i$, which comes from the fact that $\beta_2(\mu_c = M_\pi) \neq 0$ for $a_1 = \hat{q}_i = 0$, with β_2 in (67) due to the linear term contribution. That is, taking into account also the results in Sec. IV A, the presence of the linear term implies that the conditions $n_I(\mu_I < \mu_c) = 0$ and $\mu_\pi = M_\pi$ can be mutually satisfied at NLO only if the new terms considered here are taken into account. Recall that in previous ChPT studies [21,22], those conditions hold but the linear term was not considered.

As explained in Sec. III A, $\mu_c \neq M_\pi$ is theoretically allowed when interactions are included within the most general effective Lagrangian formalism, and is indeed consistent with the lattice. Nevertheless, we will evaluate numerically the different observables to NLO in the following section with and without using the constraint (69), which physically amounts to imposing that the system still behaves as a noninteracting Bose gas as far as the critical point is concerned. In any case, deviations will be small, consistent with (68).

V. NUMERICAL RESULTS

We will consider now the NLO evolution of chiral observables for nonzero μ_I, regarding in particular the role of the $\hat{q}_i^r$ LEC and the comparison with lattice analyses. From the results in the previous sections, we see that the NLO free energy density depends on seven independent new LECs, namely, $a_1, \hat{q}_{1-6}^r$ whose numerical values will then influence the μ_I dependence of the observables. Note that all the observables considered depend on $\hat{q}_{1-6}^r$ since, in addition to the explicit $\hat{q}_i^r$ dependence, one must consider that in $\alpha_0^{\rm NLO}$. We will represent our results for the range of natural values (51) at the scale $\mu = M_\rho$ and setting $a_1 = -0.019$ (the mean value obtained in fit 3 in Sec. III B). Thus, we have 3^6 points for each μ_I, corresponding to the three values $0, \pm 1/(16\pi^2)$. In doing so, we discard those $\hat{q}_i^r$ violating the condition (61), and we calculate the mean square error of the results which provides a dispersion estimation. Note that, as commented in Sec. III C 3, due to the linear term, the minimum could disappear above a given μ_I. Thus, the uncertainty bands in the following figures for a given $\mu_I > \mu_c$ correspond to those $\hat{q}_i^r$ combinations for

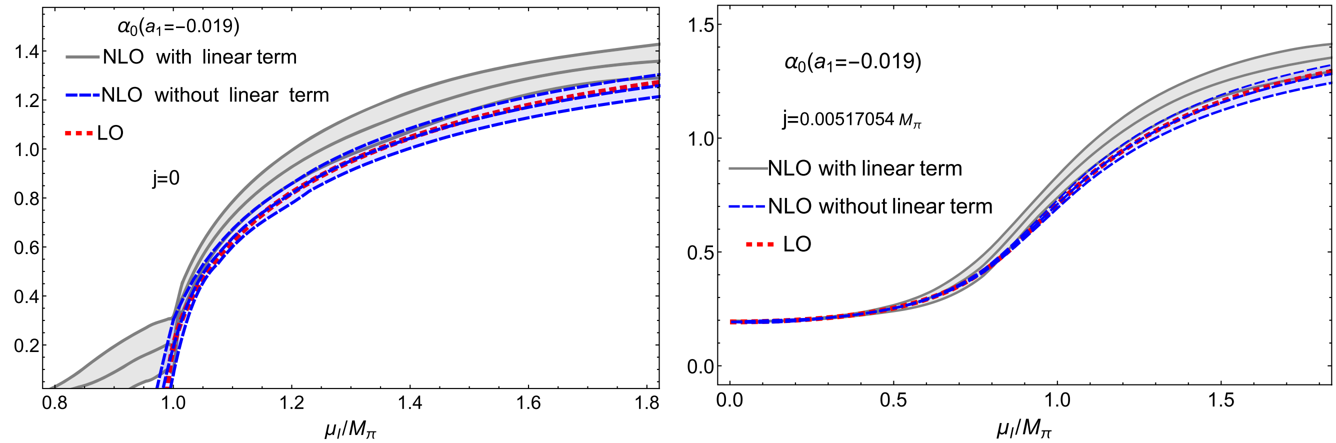

FIG. 7. Results for the minimizing angle α_0 at NLO for finite source $j = 0$ (left) and $j = 0.005170554 M_\pi$ (right), with $a_1 = -0.019$ and natural values for $\hat{q}^r_{1-6}$. The LO refers to $\alpha_0^{(2)}$ in (22).

which the minimum exists. The effect of the linear term will be actually shown separately in the figures in order to calibrate better its effect. In addition, as we have just mentioned in Sec. IV B, we will show separately the results with and without imposing the NLO condition $\mu_c = M_\pi$ in (69). For an easier comparison with our analysis in previous sections, we also plot in the following figures the curves obtained in the fit of Sec. III B, which we denote as LO, although, as commented above, they contain a_1 which is formally a NLO contribution.

First, in Fig. 7, we show $\alpha_0^{\rm NLO}$, i.e., the angle minimizing the free energy density including NLO corrections. We see that including all the corrections discussed here implies sizable deviations above μ_c with respect to the LO, larger than in previous analyses [21,22]. Note in particular the tail below $\mu_I = M_\pi$ coming from the reduction in the numerical value of $\mu_c^{\rm NLO}$ as Table II shows.

We plot in Fig. 8 the quark and pion condensate deviations (as defined in [22]) at NLO for natural values of $\hat{q}^r_i$ with and without a linear term, comparing with lattice results. The NLO corrections are again significant and remain within the uncertainties of lattice points, taking into account that we are not performing a complete NLO fit with all the free parameters, so there would be still room for improvement. For high μ_I values, the NLO corrections actually improve over the LO fit in Sec. III B for the pion condensate, whereas in the case of the quark condensate, with the inclusion of the linear term, the theoretical curve seems to depart from the lattice points with respect to the LO.

Finally, we study the isospin density at NLO for $j = 0$. The result, including the uncertainty bands of $\hat{q}^r_i$ natural values, is shown in Fig. 9. As for previous observables, the NLO with the new terms considered in this work provides

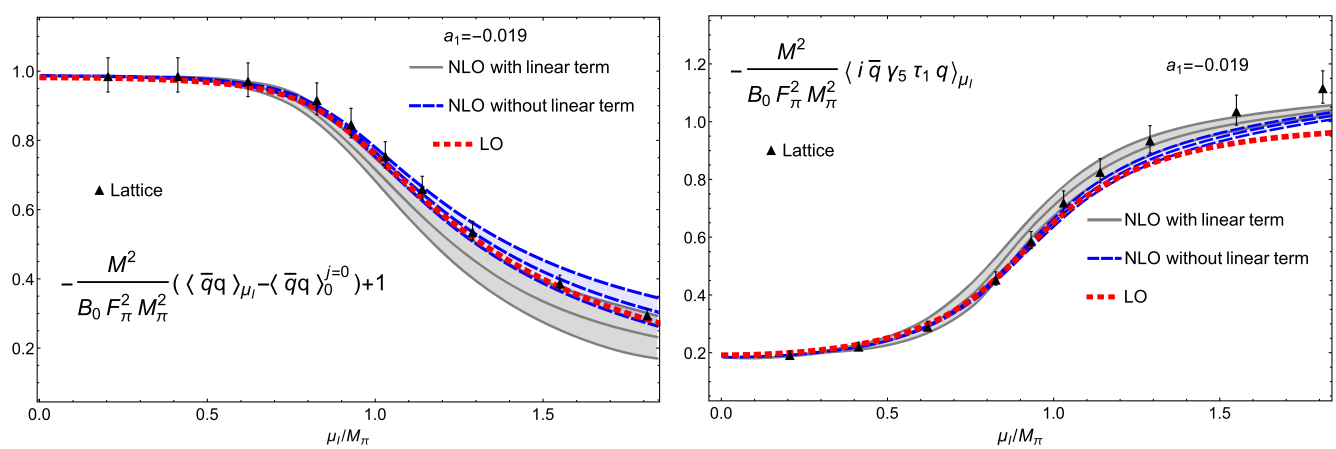

FIG. 8. Results for the quark condensate deviation (left) and pion condensate deviation (right) as a function of μ_I/M_π at NLO for finite source $j = 0.005170554 M_\pi$, $a_1 = -0.019$, and natural values for $\hat{q}^r_i$. The lattice data are from [22]. The LO refers to $\langle \bar{q}q\rangle^{(2)}$ and $\langle i\bar{q}\gamma_5\tau_1 q\rangle^{(2)}$ in (33) and (34), respectively.

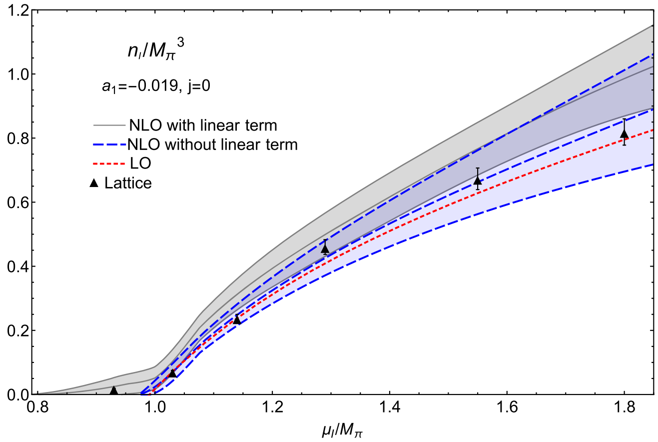

FIG. 9. Normalized isospin density as a function of μ_I/M_π at NLO with and without the linear term. Lattice points are taken from [38]. The LO refers to $n_I^{(2)}$ in (35).

significant deviations from the LO as μ_I increases, still accommodating the lattice results.

As explained above, for the NLO analysis we have fixed a_1 to the LO fit and consider the new $\hat{q}_i^r$ within natural values. In view of the results in Figs. 8 and 9, we would surely have obtained a much better description of lattice results by keeping a_1 and the $\hat{q}_i^r$ as fit parameters with the NLO curves, but such a precision analysis is outside the scope of this work.

Finally, in Fig. 10 we show the same observables as in Figs. 8 and 9 but using Eq. (69) to fix $\mu_c = M_\pi$ and eliminate the constant $\hat{q}_3^r$ in terms of a_1, $\hat{q}_2^r$, and $\hat{q}_6^r$. The pion and quark condensate corrections at NLO fixing $\mu_c = M_\pi$ remain very close to the corrections calculated without setting the critical value and, as in that case, most of the lattice data fall into the uncertainty bands. As for the isospin density, fixing $\mu_c = M_\pi$ narrows the uncertainty band around the pion mass since n_I vanishes in that case below M_π, remaining compatible with lattice data except for the lattice point below M_π.

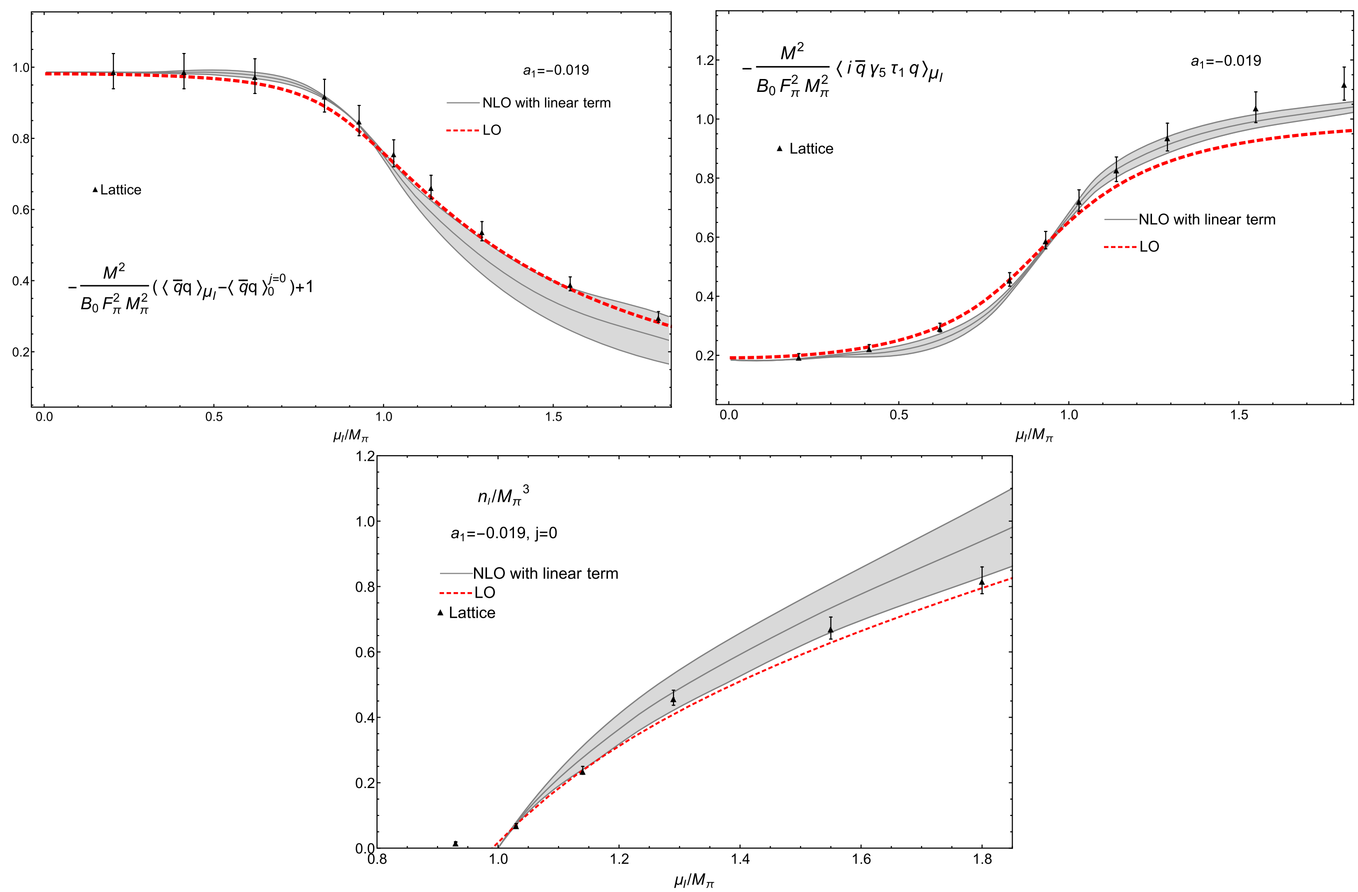

FIG. 10. Results for the quark condensate (upper left panel), pion condensate (upper right panel), and isospin density (lower panel) deviations as a function of μ_I/M_π at NLO for $a_1 = -0.019$ and fixing $\mu_I = M_\pi$. We show the expected uncertainty bands within the range of natural values for $\hat{q}^r_{1,2,4,5,6}$ and $\hat{q}_3^r$ fixed by the constraint given in (69). The value of j for the quark and pion condensates is the same as in Fig. 8. The lattice data are from [22]. The LO refers to $\langle \bar{q}q\rangle^{(2)}$, $\langle i\bar{q}\gamma_5\tau_1 q\rangle^{(2)}$, and $n_I^{(2)}$.

VI. CONCLUSIONS

In the present work, we have analyzed the most general effective chiral Lagrangian for nonzero isospin chemical potential for two light flavors up to $\mathcal{O}(p^4)$. We have followed the technique of external sources including spurion fields, which allows us to account for all possible operators respecting the symmetry-breaking problem at hand. The effect of the new Lagrangian terms in the free energy density has been calculated up to next-to-leading order. In addition, we have calculated a new NLO contribution to the free energy density coming from terms linear in the pion fields.

In the second-order Lagrangian $\mathcal{L}_2$, two new independent terms have to be considered, whose corresponding low-energy constants a_1, a_2 are related from the constraint of vanishing isospin density below the critical BEC value μ_c. The constant a_1 contributes in particular to a shift in μ_c with respect to the pion mass, although our complete NLO analysis shows that parametrically $\mu_c = M_\pi$ still holds at leading order. To estimate the preferred value of a_1, we have performed several fits to lattice results for the quark and pion condensates (for nonzero pionic source j) as well as for the isospin density (for $j = 0$), which favor $a_1 < 0$ (and therefore, $\mu_c < M_\pi$) with $|a_1| \ll 1$, consistent with its parametric NLO dependence. When comparing to the $a_1 = 0$ results, a small nonzero negative value for a_1 improves the description of lattice results, especially for the isospin density.

The $\mathcal{O}(p^4)$ Lagrangian $\mathcal{L}_4$ contains seven new terms with new low-energy constants $\hat{q}_i$, which we have consistently renormalized to absorb the divergences coming from loops with vertices of the new $\mathcal{L}_2$ terms. As mentioned above, the NLO free energy density includes also an additional contribution coming from a term in $\mathcal{L}_2$ linear in the pion fields. That term comes from the NLO corrections to the angle minimizing the free energy density. The effect of the linear term is qualitatively important, since it eventually makes the minimum of the free energy density disappear, which sets a natural limit of validity for the ChPT framework consistent with lattice analyses.

Imposing that the isospin density vanishes below μ_c to NLO gives rise to additional constraints, involving now the $a_1, a_2, \hat{q}_i^r$ LECs. Those constraints imply, on the one hand, that the $a_{1,2}$ contributions belonging are parametrically to the NLO, consistent with the small value for a_1 found in our fits. On the other hand, the dependence on one of the seven new LECs can be eliminated. In addition, the critical BEC value to NLO must remain below the LO one, which restricts further the admissible values for the $\hat{q}_i^r$. If $\mu_c = M_\pi$ is demanded also to NLO, a further constraint arises, which could not be satisfied if all the new LECs would vanish, due to the correction to μ_c coming from the linear term.

We have estimated the effect of the new LECs and the linear term to NLO by keeping the $\hat{q}_i^r$ within natural values and using for a_1 our fitted value. The results for the different observables show again consistency with the lattice points, leaving room for improvement with respect to the LO within the $\hat{q}_i^r$ uncertainty.

In summary, our present analysis has established systematically the most general way to describe low-energy QCD at nonzero isospin density, consistent with lattice results and complementing previous theoretical analyses. We believe that this work will be useful toward a better understanding of the QCD phase diagram, and we leave for future works its extension to three flavors and finite temperature.

ACKNOWLEDGMENTS

This work is partially supported by Research Contract No. PID2019–106080 GB-C21 (Spanish "Ministerio de Ciencia e Innovación"), and the European Union Horizon 2020 research and innovation program under Grant Agreement No. 824093. A. V.-R. acknowledges support from a fellowship of the UCM predoctoral program.

[1] Y. Aoki, S. Borsanyi, S. Durr, Z. Fodor, S. D. Katz, S. Krieg, and K. K. Szabo, J. High Energy Phys. 06 (2009) 088.
[2] S. Borsanyi, Z. Fodor, C. Hoelbling, S. D. Katz, S. Krieg, C. Ratti, and K. K. Szabó (Wuppertal-Budapest Collaboration), J. High Energy Phys. 09 (2010) 073.
[3] A. Bazavov *et al.* (HotQCD Collaboration), Phys. Rev. D **90**, 094503 (2014).
[4] A. Bazavov *et al.* (HotQCD Collaboration), Phys. Lett. B **795**, 15 (2019).
[5] C. Ratti, Rep. Prog. Phys. **81**, 084301 (2018).
[6] A. Bazavov, F. Karsch, S. Mukherjee, and P. Petreczky (USQCD Collaboration), Eur. Phys. J. A **55**, 194 (2019).
[7] L. Adamczyk *et al.* (STAR Collaboration), Phys. Rev. C **96**, 044904 (2017).
[8] A. Andronic, P. Braun-Munzinger, K. Redlich, and J. Stachel, Nature (London) **561**, 321 (2018).
[9] M. D'Elia and M. P. Lombardo, Phys. Rev. D **67**, 014505 (2003).
[10] P. de Forcrand and O. Philipsen, J. High Energy Phys. 01 (2007) 077.
[11] Z. Fodor and S. D. Katz, J. High Energy Phys. 04 (2004) 050.
[12] G. Aarts, Phys. Rev. Lett. **102**, 131601 (2009).
[13] A. Bazavov *et al.*, Phys. Rev. Lett. **113**, 072001 (2014).
[14] A. Yamamoto, Phys. Rev. D **84**, 114504 (2011).

[15] V. V. Braguta, E. M. Ilgenfritz, A. Y. Kotov, B. Petersson, and S. A. Skinderev, Phys. Rev. D **93**, 034509 (2016).
[16] N. Y. Astrakhantsev, V. V. Braguta, A. Y. Kotov, D. D. Kuznedelev, and A. A. Nikolaev, Eur. Phys. J. A **57**, 15 (2021).
[17] A. A. Andrianov, D. Espriu, and X. Planells, Eur. Phys. J. C **73**, 2294 (2013).
[18] D. Espriu, A. Gómez Nicola, and A. Vioque-Rodríguez, J. High Energy Phys. 06 (2020) 062.
[19] D. E. Kharzeev, Prog. Part. Nucl. Phys. **75**, 133 (2014).
[20] D. T. Son and M. A. Stephanov, Phys. Rev. Lett. **86**, 592 (2001).
[21] P. Adhikari, J. O. Andersen, and P. Kneschke, Eur. Phys. J. C **79**, 874 (2019).
[22] P. Adhikari and J. O. Andersen, Eur. Phys. J. C **80**, 1028 (2020).
[23] P. Adhikari, J. O. Andersen, and M. A. Mojahed, Eur. Phys. J. C **81**, 449 (2021).
[24] S. Carignano, L. Lepori, A. Mammarella, M. Mannarelli, and G. Pagliaroli, Eur. Phys. J. A **53**, 35 (2017).
[25] W. Detmold, K. Orginos, and Z. Shi, Phys. Rev. D **86**, 054507 (2012).
[26] M. Loewe and C. Villavicencio, Phys. Rev. D **67**, 074034 (2003).
[27] E. S. Fraga, L. F. Palhares, and C. Villavicencio, Phys. Rev. D **79**, 014021 (2009).
[28] T. D. Cohen and S. Sen, Nucl. Phys. **A942**, 39 (2015).
[29] P. Adhikari, J. O. Andersen, and M. A. Mojahed, Eur. Phys. J. C **81**, 173 (2021).
[30] K. Splittorff, D. T. Son, and M. A. Stephanov, Phys. Rev. D **64**, 016003 (2001).
[31] P. Adhikari and J. O. Andersen, J. High Energy Phys. 06 (2020) 170.
[32] J. B. Kogut and D. Toublan, Phys. Rev. D **64**, 034007 (2001).
[33] Z. Y. Lu, C. J. Xia, and M. Ruggieri, Eur. Phys. J. C **80**, 46 (2020).
[34] J. B. Kogut and D. K. Sinclair, Phys. Rev. D **70**, 094501 (2004).
[35] P. de Forcrand, M. A. Stephanov, and U. Wenger, Proc. Sci., LATTICE2007 (**2007**) 237, arXiv:0711.0023.
[36] B. B. Brandt and G. Endrodi, Proc. Sci., LATTICE2016 (**2016**) 039.
[37] B. B. Brandt, G. Endrodi, and S. Schmalzbauer, Phys. Rev. D **97**, 054514 (2018).
[38] B. B. Brandt, G. Endrodi, E. S. Fraga, M. Hippert, J. Schaffner-Bielich, and S. Schmalzbauer, Phys. Rev. D **98**, 094510 (2018).
[39] P. Adhikari and J. O. Andersen, Phys. Lett. B **804**, 135352 (2020).
[40] B. S. Lopes, S. S. Avancini, A. Bandyopadhyay, D. C. Duarte, and R. L. S. Farias, Phys. Rev. D **103**, 076023 (2021).
[41] J. Gasser and H. Leutwyler, Ann. Phys. (N.Y.) **158**, 142 (1984).
[42] J. Gasser and H. Leutwyler, Nucl. Phys. **B250**, 465 (1985).
[43] G. Ecker, J. Gasser, A. Pich, and E. de Rafael, Nucl. Phys. **B321**, 311 (1989).
[44] R. Urech, Nucl. Phys. **B433**, 234 (1995).
[45] U. G. Meissner, G. Muller, and S. Steininger, Phys. Lett. B **406**, 154 (1997); **407**, 454(E) (1997).
[46] M. Knecht and R. Urech, Nucl. Phys. **B519**, 329 (1998).
[47] S. Scherer, Adv. Nucl. Phys. **27**, 277 (2003).
[48] D. Espriu, E. de Rafael, and J. Taron, Nucl. Phys. **B345**, 22 (1990); **B355**, 278(E) (1991).
[49] G. Colangelo, J. Gasser, and H. Leutwyler, Nucl. Phys. **B603**, 125 (2001).